2023

Androgen Receptor Inhibition Suppresses Anti-Tumor Neutrophil Response Against Bone Metastatic Prostate Cancer via Regulation of TβRI Expression

Massar Alsamraae

Diane Costanzo-Garvey

Benjamin A. Teply

Shawna Boyle

Gary Sommerville

See next page for additional authors

Authors

Massar Alsamraae, Diane Costanzo-Garvey, Benjamin A. Teply, Shawna Boyle, Gary Sommerville, Zachary T. Herbert, Colm Morrissey, Alicia J. Dafferner, Maher Y. Abdalla, Rachel W. Fallet, Tammy Kielian, Heather Jensen Smith, Edson I. deOliveira, Keqiang Chen, Ian A. Bettencourt, Ji Ming Wang, Daniel W. McVicar, Tyler Keeley, Fang Yu, and Leah M. Cook

Cancer Letters 579 (2023) 216468

Contents lists available at ScienceDirect

Cancer Letters

journal homepage: www.elsevier.com/locate/canlet

Androgen receptor inhibition suppresses anti-tumor neutrophil response against bone metastatic prostate cancer via regulation of TβRI expression

Massar Alsamraae [a,1], Diane Costanzo-Garvey [a,1], Benjamin A. Teply [b,c], Shawna Boyle [b], Gary Sommerville [d], Zachary T. Herbert [d], Colm Morrissey [e], Alicia J. Dafferner [a], Maher Y. Abdalla [a], Rachel W. Fallet [a], Tammy Kielian [a], Heather Jensen-Smith [b,f], Edson I. deOliveira [a], Keqiang Chen [g], Ian A. Bettencourt [g], Ji Ming Wang [g], Daniel W. McVicar [g], Tyler Keeley [a], Fang Yu [h], Leah M. Cook [a,b,*]

[a] Department of Pathology and Microbiology, University of Nebraska Medical Center, Omaha, NE, USA
[b] Fred & Pamela Buffett Cancer Center, Omaha, NE, USA
[c] Division of Oncology & Hematology/Oncology, Department of Internal Medicine, University of Nebraska Medical Center Omaha, NE, USA
[d] Dana Farber Cancer Institute, Boston, MA, USA
[e] University of Washington, Seattle, WA, USA
[f] Eppley Institute for Research in Cancer and Allied Diseases, Omaha, NE, USA
[g] Laboratory of Cancer Innovation, National Cancer Institute, Frederick, MD, USA
[h] Department of Biostatistics, University of Nebraska Medical Center, Omaha, NE, USA

A B S T R A C T

Bone metastatic disease of prostate cancer (PCa) is incurable and progression in bone is largely dictated by tumor-stromal interactions in the bone microenvironment. We showed previously that bone neutrophils initially inhibit bone metastatic PCa growth yet metastatic PCa becomes resistant to neutrophil response. Further, neutrophils isolated from tumor-bone lost their ability to suppress tumor growth through unknown mechanisms. With this study, our goal was to define the impact of metastatic PCa on neutrophil function throughout tumor progression and to determine the potential of neutrophils as predictive biomarkers of metastatic disease. Using patient peripheral blood polymorphonuclear neutrophils (PMNs), we identified that PCa progression dictates PMN cell surface markers and gene expression, but not cytotoxicity against PCa. Importantly, we also identified a novel phenomenon in which second generation androgen deprivation therapy (ADT) suppresses PMN cytotoxicity via increased transforming growth factor beta receptor I (TβRI). High dose testosterone and genetic or pharmacologic TβRI inhibition rescued androgen receptor-mediated neutrophil suppression and restored neutrophil anti-tumor immune response. These studies highlight the ability to leverage standard-care ADT to generate neutrophil anti-tumor responses against bone metastatic PCa.

1. Introduction

Prostate cancer (PCa) is the second most common cause of cancer death among men in the United States, accounting for an estimated 34,000 cancer deaths in 2023, which are mostly associated with metastatic disease [1,2]. The current standard of therapy for advanced prostate cancer is either prostatectomy or initial androgen deprivation therapy (ADT), with response to therapy being initially characterized by biochemical response i.e., changes in the levels of prostate-specific antigen (PSA) [3,4]. Approximately 50 % of PCa patients progress to advanced stage disease characterized by biochemical recurrence and often, progression to metastatic disease or metastatic castration-resistant prostate cancer (mCRPC) [5] which is incurable. Although mCRPC patients exhibit progressing disease, many will initially respond to additional androgen receptor (AR) directed therapy given in the form of more selective androgen inhibitors including, inhibitors of androgen synthesis and AR signaling, such as abiraterone acetate (which inhibits CYP17A1) and enzalutamide, respectively [6–8]. However, even with a ~4–6 month improvement in overall survival, mCRPC patients typically succumb to the disease within 3 years after diagnosis of metastases. These statistics demonstrate a significant need to identify additional therapies or personalized therapeutic approaches.

Bone is the most frequent tissue site for metastatic PCa. It has been classically shown that within the bone microenvironment PCa promotes

* Corresponding author. Dept. of Pathology/Microbiology, University of Nebraska Medical Center, 985900 Nebraska Med Center, Omaha, NE, 68198, USA.
E-mail address: leah.cook@unmc.edu (L.M. Cook).
[1] Designates equal contribution.

https://doi.org/10.1016/j.canlet.2023.216468
Received 14 July 2023; Received in revised form 19 October 2023; Accepted 27 October 2023
Available online 7 November 2023

bone remodeling, e.g., excessive bone degradation, which subsequently releases bone-sequestered growth factors such as transforming growth factor beta, TGFβ, and further promotes tumor growth in what has been characterized as a "vicious" cycle of continued bone remodeling and cancer growth in bone [9,10]. Importantly, PCa interactions with bone stromal cells contribute significantly to the progression of bone metastatic PCa (BM-PCa). We recently identified that bone marrow neutrophils and neutrophil precursors, which account for ~50–60 % of cells in bone marrow [11,12], migrate to BM-PCa and are protective against PCa growth in bone. Further, we found that BM-PCa resists neutrophil anti-tumor response and suppresses neutrophil cytotoxicity as the tumor progresses. However, the role of neutrophils in the progression of BM-PCa remains unclear.

Neutrophils are the most abundant leukocyte population in blood, representing 50–70 % of all immune cells. More than 10^{11} neutrophils are produced daily in bone marrow and released into circulation, ready to elicit an innate immune response to pathogens and tissue damage. Based on evidence from our lab suggesting that the PCa tumor-bone environment suppresses neutrophil function, we sought to determine whether neutrophils might be utilized as biomarkers of disease progression and therapeutic response, and for identifying the impact of prostate cancer disease stage on neutrophil immune response.

In this study, we utilized patient-derived PMNs for comparison to primary bone marrow neutrophils and ran a preclinical mouse trial which revealed several novel insights into neutrophils in PCa. Importantly, we observed a therapy-associated regulation of neutrophil cytotoxicity that was independent of disease stage and the tissue source of neutrophils. Therapeutic options are limited for BM-PCa patients and in this study, we identified: 1) a novel mechanism through which androgens regulate neutrophil function and 2) PCa-associated neutrophil properties that can be utilized for development of neutrophil-focused cancer immunotherapy.

2. Materials & methods

Patient samples. *Prospective blood sample collection:* Healthy men and PCa patients were deemed eligible and consented for sample donation within the UNMC integrated Cancer Repository for Cancer Research (iCaRe2). The iCaRe2 is a multi-institutional resource created and maintained by the Fred & Pamela Buffett Cancer Center to collect and manage standardized, multi-dimensional, longitudinal data and biospecimens on consented adult cancer patients, high-risk individuals, and normal controls. Patients for this study were specifically recruited from the Genitourinary Cancer Registry (GU-CARE), and all samples collected prospectively under the guidance and approval of the UNMC Institutional Review Board (IRB) and under iCaRe2 during routine patient appointments. The study consisted of 4 groups (n= >17/group): 1) healthy (no cancer or pathological disease) (n = 17), 2) localized PCa (n = 22), 3) bone metastatic hormone-/castration-sensitive PCa (mCSPC) (n = 19), and 4) bone metastatic castration-resistant PCa (mCRPC) (n = 19). PCa patients in our study received treatments according to the National Comprehensive Cancer Network (NCCN) guidelines, including androgen deprivation therapy (ADT): Leuprolide (1st line ADT group), AR signaling inhibitors (ARSIs; abiraterone, enzalutamide, darolutamide, apalutamide), and chemotherapy (docetaxel). Some patients received bone-targeted radiation therapy, radium-223. Patient blood was collected and PMNs immediately isolated after collection and utilized for downstream analyses, including cell counts, viability, flow cytometry, RNA and protein collection, RNA sequencing, and co-culture assay. Although one patient presented with additional malignancies, the co-culture data in this manuscript includes only bone metastatic patients. *FFPE Rapid Autopsy samples:* FFPE prostate metastases were provided from patients who signed written informed consent under the aegis of the Prostate Cancer Donor Program at the University of Washington (IRB protocol # 2341).

Mice. Only male mice were used for these studies. For neutrophil isolations, C57BL/6 mice were utilized (Jackson Laboratory; # 000664). Mice (8–12 weeks) were used for all experiments using mouse primary neutrophils. C57BL/6 males (6 weeks of age) were used for RM1 *in vivo* intratibial metastasis models. For human PCa cell intratibial metastasis models, immunocompetent SCID/Beige (C·B-17/IcrHsd-Prkdcscid-Lystbg-J) mice were utilized (6 weeks, Envigo). $T\beta RI^{flox/flox}$ mice were purchased (Jackson Laboratory; #028701) and backcrossed 8 times to C57BL/6 to obtain a pure background. To generate neutrophil-selective *TβRI* knockout mice, Catchup mice [13] ($Ly6G^{Cre/dtom}$) were crossed with $T\beta RI^{flox/flox}$ mice; knockout $T\beta RI^{-/-}$ was determined using PCR genotyping and confirmed using immunoblot protein analysis of mouse tissues. Mice were housed on a 12 h light/dark cycle, with free access to food and water. All procedures performed were approved by IACUC (UNMC).

Cell culture media and reagents. LNCaP cells were cultured in RPMI complete media (RPMI (Hyclone), 10 % FBS (Peak Serum), and 1 % penicillin/streptomycin (Gibco)). C42B, PC3, and RM1 were cultured in DMEM complete media (DMEM (Hyclone), 10 % FBS (Peak Serum), and 1 % penicillin/streptomycin). To collect conditioned media (CM), cell lines were washed with Phosphate Buffered Saline (PBS) to remove serum, full medium was replaced with serum-free medium RPMI and cells were incubated for 24 h. CM was collected and centrifugation was done to remove cellular debris and stored at 4 °C until usage. Total protein content of CM was measured using BCA assay (ThermoFisher) to ensure equal protein concentrations for treating neutrophils. Fresh media was collected every 2 weeks for experimental use.

Neutrophil isolation. From patients, polymorphonuclear leukocytes/neutrophils (PMNs) neutrophils were isolated from freshly collected blood, within 5 h of collection. Neutrophils were isolated using a commercially available kit (Human-EasySep Neutrophil Isolation, StemCell; Mouse-MojoSort Neutrophil Isolation, Biolegend), that involves negative selection from other cells using magnetic beads. PMNs were isolated specifically using a negative isolation magnetic bead method to prevent premature activation. Purity was confirmed by flow cytometry for cell surface markers (Human-$CD14^-$, $CD15^+$, $CD16^+$, $CD66b^+$; Mouse-$CD11b^+Ly6G^+$) and morphology assessment using Giemsa stain, as described [14–16]. For mouse tumor-associated neutrophils (TANs) and primary neutrophil co-cultures, bone marrow neutrophils were isolated from mouse tibia and femurs of male C57BL/6 mice. Bones were cleared of tissue and muscle, and the epiphysis was removed and discarded. A hole was made in the bottom of a 0.65 mL tube, and one bone was placed individually per tube. This tube was placed into a 1.5-mL tube for bone marrow collection, where it was then centrifuged at high speed for for ~5 s. The bone marrow was re-suspended in 1 mL of neutrophil isolation buffer and filtered using a 70 μm filter. Bones from each mouse were pooled and counted, and the MojoSort Neutrophil Enrichment (Biolegend) protocol was followed, as per manufacturers' instructions. Neutrophil isolation buffer used for isolations consists of: 1X PBS, 2 % FBS and 2 mM EDTA. All *in vitro* assays (viability analysis, flow cytometry, co-culture) were setup and/or performed immediately. Patient PMN protein and RNA were isolated immediately after PMN isolation from blood and stored at −80 °C for downstream analyses.

Real-time Glo MT cell viability assay. PMNs were incubated in triplicate at 100,000 per well in PCa CM with 2x Real-Time Glo reagent (Promega). MT Cell Viability Substrate and NanoLuc® Enzyme were added in equal volumes to culture media to create the 2x Real-time Glo reagent. This media was added directly to the cells at time zero, and luminescence was read at the indicated time points using a luminometer. Mouse neutrophils were treated for 2 h with media supplemented with enzalutamide (Selleckchem) at 3 μM and 10 μM, then luciferase was quantified.

Flow cytometry. From patient samples, isolated peripheral blood neutrophils were washed and reconstituted in FACS buffer (2 % FBS in 1X PBS) at 1×10^6 cells in 200 μL. For tumor studies, bone marrow was flushed from tumor-bearing and saline-injected tibiae using a syringe

and excess cells were further flushed out of the marrow with FACS buffer. For staining, cells were incubated on ice with fluorophore-conjugated antibodies added at a maximum of 1 μL per 10^6 cells in appropriate antibodies listed in Supplemental Table 1. Cell viability dye, Live/Dead (Invitrogen), was also added at a concentration of 0.2 μL per 10^6 cells. Stained cells were incubated with antibody on ice in the dark for 20 min, rinsed with 1X PBS and were fixed in 1 % formaldehyde in 1XPBS for 30 min in the dark. Prior to analysis, cells were reconstituted in FACS buffer. For all analyses, single and live cells were gated and percentage of positive cells per marker was quantified (FACS Diva software, LSRII, BD Biosciences).

RNA Library Preparation and Bulk RNA Sequencing. For patient samples, peripheral blood neutrophils were isolated and reconstituted in Trizol reagent. RNA was purified from Trizol using DirectZol kit (Zymogen), according to manufacturer instructions. Libraries were prepared using RiboErase and RNA HyperPrep sample preparation kits (Roche Kapa Biosystems) from 100 ng of RNA. RNA samples were fragmented at 94C for 8 min with 14 cycles of PCR post-adapter ligation according to manufacturer's recommendation. The finished dsDNA libraries were quantified by Qubit fluorometer and Agilent TapeStation 2200. Libraries were pooled in equimolar ratios and evaluated for cluster efficiency and pool balance with shallow sequencing on an Illumina MiSeq. Final sequencing was performed on an Illumina NovaSeq with paired-end 100bp reads at the Dana-Farber Cancer Institute Molecular Biology Core Facilities. *RNASeq Analysis*. Sequenced reads were aligned to the UCSC hg38 reference genome assembly and gene counts were quantified using STAR (v2.7.3a) [17]. Differential gene expression testing was performed by DESeq2 (v1.22.1) [18]. Initial RNAseq analysis was performed using the VIPER snakemake pipeline [19]. Data was further analyzed using Ingenuity Pathway Analysis software (IPA; Qiagen). The full gene list was uploaded into the NCBI Repository and can be accessed at GEO Accession: GSE197609.

Real-time qPCR. For RNA isolation, Trizol reagent was added to treated neutrophils and RNA was extracted using the standard Trizol isolation protocol. RNA (1 μg) was used to synthesize cDNA using qSCRIPT Super mix (Quantabio) and PCR was performed using Perfecta SYBR Green FastMix (Quantabio). PCR was run using Bio-Rad CFX Real-Time System. PCR conditions were as follows for all primer sequences (Integrated DNA Technologies; sequences listed in **Supplemental Table 2**): Step 1: 95° 30s; Step 2: 95° 5s, 57° 15s, 72° 10s, 95° 10s (× 39 cycles); Step 3: Melt curve 65°–95° at increments of 0.5° for 5s. For enzalutamide experiments: mouse primary bone marrow neutrophils were treated with 3 μM and 10 μM enzalutamide for 2 h at 37 °C in complete RPMI media and RNA isolated using Trizol.

PCa:Neutrophil Co-culture assay. For PCa co-cultures with neutrophils, PCa cells were plated at 30,000 cells/well in a 24-well plate, in triplicate per condition. Twenty-four hours later, neutrophils were isolated, re-suspended in complete medium, and plated in direct contact with cancer cells at a ratio of 10:1 (neutrophils/cancer) and 3 μM, 10 μM enzalutamide were added into the media or neutrophils were treated with enzalutamide for 30 min prior to addition to the culture, where noted, in complete RPMI. For TβRI co-culture assays, primary neutrophils were incubated in complete RPMI supplemented with RepSox (5 nM; Selleckchem) in the presence or absence of enzalutamide, for 30 min prior to addition to PCs cells. After incubation overnight, neutrophils were removed, and cancer cell viability was measured with Trypan Blue Exclusion assay, using a hemacytometer.

Neutrophil Extracellular Trap (NET) Production assay. For analysis of PMN NET secretion, primary mouse neutrophils were incubated for 2 h in prostate CM (LNCaP, C42B) with or without enzalutamide (3 μM) or complete RPMI supplemented with PMA (100 nM) as a positive control. Sytox Green dye (500 nM; Sigma) was added to each condition, and after 30 min, images were taken of each well by an EVOS FL Auto microscope (Invitrogen; AMAFD1000). The number of green fluorescent DNA traps/NETs was measured as a percentage of total cells to distinguish between dying cells that absorbed the Sytox Green dye. CM-treated neutrophils were compared to neutrophils incubated in serum-free media RPMI.

Neutrophil migration assay. Primary neutrophils were isolated from mouse hind limbs using MojoSort and 1×10^5 seeded in the top of transwell migration chambers, with a pore size of 5 μm (Costar; Ref # 3422). Neutrophils were allowed to migrate towards prostate cancer CM added to the bottom of the respective wells for 1 h. To examine impact of androgen signaling, mouse neutrophils were pre-treated with 3 μM of enzalutamide or abiraterone (R&D Systems) for 30 min before addition the insert. Neutrophils were allowed to migrate towards specific conditions for 1 h: serum-free media, serum containing 2 % FBS, LNCaP CM, and C42B CM. Inserts were fixed in 100 % methanol for 5 min, washed in 1X PBS to remove non-adherent cells and stained with hematoxylin for quantitation of the number of migrating neutrophils per insert. Insert membranes were mounted on a slide using Permount (Fisher Scientific) and imaged using an EVOS FL Auto microscope at 10× magnification.

Immunoblot analysis. Protein was isolated from patient PMNs using RIPA buffer (Thermofisher, MA) and total protein quantified using BCA assay (Pierce, Thermofisher, MA). Protein (50 μg) was run on a 12 % SDS gel and then transferred to a PVDF membrane. The membrane was stained with 0.1 % (w/v) Ponceau S in 5 % (w/v) acetic acid for 5 min at room temperature. Background staining was removed with 3 washes of distilled water prior to capturing an image. Distilled water was used to destain the membrane, non-specific binding was blocked with 5 % non-fat milk in 1X TBST for 1 h at room temperature followed by overnight incubation with the primary antibody, 1:1000 in 5 % non-fat milk, at 4 °C. The following primary antibodies were used: MnSOD (#06–984, MilliporeSigma, Burlington MA), Catalase (#ab76024, Abcam, Boston MA), CuZnSOD/SOD1 (#ab51254, Abcam, Boston MA), GAPDH (#sc-32235, Santa Cruz Biotechnology, Dallas TX). The blot was washed in TBST prior to incubating with the secondary antibody, 1:4700 in 5 % non-fat milk (anti-rabbit IgG #ADI-SAB-300-J, Enzo Lifesciences, Farmingdale NY or anti-mouse IgG #7076, Cell Signaling Technology, Danvers MA). The membranes were imaged using Azure Biosystems Radiance Plus substrate solution and an Azure c600 Imaging System.

Immunohistochemistry. Patient bone specimens and mouse tibia bone sections were dewaxed and hydrated through an alcohol gradient. Antigen retrieval for human and mouse specimens was performed using Tris-EDTA buffer (pH 9) in a pressure cooker on high temp for 6 min. Tissues were then blocked in 10 % serum in 1X tris-buffered saline (TBS) for 1 h prior to overnight incubation in primary antibodies (Myeloperoxidase (7.5 μg/ml), R&D MAB3174; TGFβ Receptor I (1:100), Millipore, ABF17-1). Following washes, species-specific secondary AlexaFluor antibodies were incubated 1:1000 on the tissues for 1 h at room temperature. Fluorescent images were taken on a Zeiss Axio Imager Z2 at 20x.

Two-photon microscopy. An upright Olympus FVMPE-RS Multiphoton Laser Scanning Microscope equipped with a Spectra Physics dual line InSight X3 near infrared laser and 25x (1.05 NA) water-immersion objective was used to image inside intact tibial bone. Collagen autofluorescence (AF, 495–540 nm emission) and second harmonic generation (SHG, 410–455 nm emission) were collected using 880 nm excitation. Fluorescence from dTomato positive PMNs was collected using 1040 nm excitation and a 575–645 nm emission filter.

Single cell RNA sequencing and data analysis. Murine bone marrow samples were used to generate 5' gene expression libraries (10x Genomics) which were sequenced on a NovaSeq 6000 instrument. Demultiplexing was performed with Bcl2fastq. Alignment, tagging, and gene and transcript counting were performed with Cellranger. Quality control and analysis were performed using the R package Seurat. Dead or low complexity cells were filtered by removing cells with less than 200 features and cells with a percentage of mitochondrial reads greater than 6 %. Doublets were removed by filtering cells with greater than 5000 features or greater than 30,000 transcripts. Filtered data was normalized with SCTransform, and dimensional reduction was performed by UMAP. Cluster ID was performed using the R package SingleR.

In vivo mouse models. Androgen regulation study: To examine the

impact of androgen regulation on tumor burden and tumor-associated bone neutrophils (TBNs) function, we performed a preclinical/mouse study using standard-of-care therapy for BM-PCa, enzalutamide, in combination with exogenous testosterone (to mimic bipolar androgen therapy (BAT)). Male SCID Beige mice were chemically castrated using subcutaneous injection once with Degarelix (commercially available gonadotropin releasing hormone antagonist; 10 mg/kg, Selleckchem) at a concentration which allowed for systemic depletion of androgen for the duration of the study [20,21]. The following day, mice were injected intratibially with luciferase-expressing C42B prostate cancer cells. For injections, C42B were grown to confluence, trypsinized and washed with 1X PBS, and filtered using a 70-μm nylon filter. Cells were counted and reconstituted for intratibial injection of 5×10^5 C42B per 40 μL volume per mouse. Mice were anesthetized with isoflurane, and 5×10^5 C42B injected into the right tibia. An equal volume of PBS was injected into the contralateral limb, as a control for the intratibial injection. At day 3 post-intratibial injection, tumor burden was imaged via bioluminescence.

For bioluminescence imaging, mice were given 10 μL/g of D-luciferin (15 mg/mL) (Gold Bio) intraperitoneally and imaged using the IVIS Spectrum imager (PerkinElmer). Luciferase signal was quantified 15 min after injection, using the Living Image Software per manufacturer's instructions. Using bioluminescence intensity, mice were randomized (based on intensity above threshold minus background signal) into 6 treatment groups (n = 4–5/group; based on available mice after confirmed tumor take) to receive either: 1) enzalutamide (10 mg/kg) or 2) vehicle control (DMSO); 3) placebo subcutaneous pellet (Innovative Research), and 4) slow-release 5-α-dihydrotestosterone pellet (DHT; 12.5 mg 21-day release; Innovative Research); 5) enzalutamide plus placebo pellet and 6) enzalutamide plus DHT pellet. Pellets were subcutaneously transplanted 7 days after the start of enzalutamide treatment. IVIS imaging was used for longitudinal measurement of tumor burden. Mice were euthanized at 2 weeks to allow for isolation of neutrophils. Tumor-bearing and saline-injected tibia were flushed with sterile PBS and neutrophils isolated using MojoSort Neutrophil Isolation kit for analysis in co-culture and for protein analysis. Protein was isolated from TBNs using RIPA Lysis buffer, total protein content measured using BCA assay, and immune-modulating cytokines and chemokines examined by protein array (RayBiotech; Mouse Cytokine Array C3), according to protocol. As a control, tumor naïve neutrophils (from tibia injected with saline) were used for comparison. Flow cytometry was performed on neutrophils from tumor bearing and tumor naïve mice using the following markers: CD11b, CD45, Ly6C, Ly6G, F4/80 and CD11c (Biolegend).

TβRI knockout and inhibitor study: To examine the impact of neutrophil-selective knockout of TβRI on BM-PCa *in vivo,* the mouse RM1 prostate cancer model was utilized; 3.5×10^4 luciferase-expressing RM1 were injected into tibia of 6–7 week old TβRI knockout ($T\beta RI^{-/-}$) or floxed TβRI mice (wildtype expression; $T\beta RI^{flox/flox}$). Additionally, luciferase-expressing RM1 was used to examine the outcome of pharmacologic TβRI and AR inhibition on PCa growth in bone. For this study, 3.5×10^5 luciferase-expressing RM1 were injected into tibia; 3 days post-injection, mice were randomized via bioluminescence into 4 treatment groups (n = 5–7/group based upon confirmation of tumor take): 1) vehicle control (DMSO), 2) enzalutamide (10 mg/kg), 3) RepSox, TβRI inhibitor (5 mg/kg), and 4) combination enzalutamide and TβRI inhibitor. After confirming the tumor take based on meeting luminescence threshold values (previously determined to reflect exponential tumor growth throughout the study), mice were randomized in drug groups based on histogram distribution compared to the median of all mice. For both studies, tumor burden was measured longitudinally throughout the study using bioluminescence and hind limbs collected at the end of the study for downstream analyses.

Statistical power and analysis. For patient samples, per power analyses for our studies by the UNMC Biostatistics Core, a minimum of 17 patients per group was needed to detect at least a 2-fold difference in gene expression. This calculation was based assumption of a sequencing depth of 20, and a coefficient of variation of 0.4, and alpha of 0.001 to adjust for multiple comparisons for the RNA-Seq study. This sample size also achieves 80 % power to detect a large Cohen's d effect size of 1.0 at alpha = 0.05 using a two-sided two-sample *t*-test. Additional subjects were recruited to account for any patients with low yields of PMN/working material. For statistical analyses: Graphpad Prism software was utilized for all other statistical analyses. Continuous patient data was compared between diagnosis and treatment groups using one way- or two-way analysis of variance (ANOVA) when appropriate. Preclinical data was analyzed using one-way ANOVA. Tukey's correction was used as a secondary test for comparing all groups to each other.

3. Results

Impact of PCa progression on PMN number and viability. Blood was prospectively isolated from men of various stages of PCa (localized/non-metastatic disease; bone metastatic hormone/castration-sensitive (mCSPC); bone metastatic castration-resistant (mCRPC). For comparison, blood was collected from healthy male donors. All patient groups and treatments are shown in Table 1. Usage of the neutrophil-to-lymphocyte ratio for determining prognosis has yielded varied results [22], thus we wanted to examine whether PMN numbers in blood are altered independently of other leukocyte populations. We found that absolute PMN numbers per volume of blood were similar between groups; however, there was a trend towards increased PMN numbers with progression to metastatic disease (comparing healthy to mCSPC) that was significantly reduced with progression from mCSPC to castration resistant disease (mCRPC) ($p < 0.01$) (Fig. 1A, left). This finding was independent of isolation-associated impact on viability as there were no significant differences noted in cell viability when comparing the three PCa groups. However, PMNs from patients with localized PCa showed increased numbers at 18 h (173 %; $p < 0.05$) and 24 h (141 %) compared to healthy patient PMNs (Fig. 1A, right), suggesting either prolonged viability or enhanced proliferation, as frequently seen with immature/undifferentiated PMNs.

PCa progression induces a pro-inflammatory PMN gene signature. To gain further insight into the impact of PCa progression on molecular changes in PMNs, we performed bulk RNA sequencing comparing disease stage (n = 16 total (4/healthy; 4/localized; 3/mCSPC; 5/mCRPC); note: we initially intended to analyze 4 per group however, one mCSPC patient became resistant to androgen therapy after diagnosis, but prior to sample collection. There were >10,000 genes detected per treatment group out of approximately 25,000 genes analyzed (full gene list can be found at GEO Accession: GSE197609) (Fig. 1B, left). Because PMNs are terminally differentiated cells, there was a low total number of genes altered per group. After controlling for the false discovery rate, we found that overall, there were more PMN genes turned "on" than "off" throughout PCa progression. When comparing disease stage, the largest number of PMN gene alterations occurred in mCRPC patients compared to healthy individuals; genes up-/down-regulated by more than 2-fold, ($p < 0.05$: 135 up/22 down; $p < 0.01$: 44 up/11 down) demonstrating that there is a change in the molecular profile of PMNs in PCa patients throughout progression. There were fewer genes altered between PCa groups and treatments (Fig. 1B, right; Supp Figs. 1A and 1B). When comparing PMNs from healthy men with CRPC patients, cancer-derived PMNs exhibited a pro-inflammatory molecular profile, including increased expression of *CD177*, *MMP8*, and *CYBB* (Fig. 1C, left). There were some shared upregulated genes, but no shared downregulated genes, when comparing mCRPC vs. healthy and the 2 metastatic groups, mCRPC vs. mCSPC, including *CYBB* (Supp Fig. 1C). There were some genes that were only altered with progression from metastatic hormone-sensitive PCa to metastatic castration-resistant disease, including complement 3 receptor 1 (*C3AR1*) and C-type Lectin Receptors 12A & 12B (*CLEC12A/12B*), which are all major inducers of inflammation suggesting a stage-

Table 1
Patient diagnosis and treatment demographics.

	n	1st Line ADT	2nd Gen ADT	Chemotherapy (Docetaxel)	ADT[b]Radium 223	Survivorship/no longer on therapy
Healthy	17	*n/a*				
Localized	22[a] [b]	4	8			9
Metastatic castration-sensitive prostate cancer (mCSPC)	19	5	12	2		
Metastatic castration-resistant prostate cancer (mCRPC)	19	4[c]	9	3	2	

[a] Includes one patient on ADT and immune checkpoint blockade (ICB).
[b] Includes one patient on ICB with other malignancies; this data was included in neutrophil counts, viability, and cell surface markers but was excluded from co-culture and sequencing analyses.
[c] Excludes one patient on ADT with evidence of other malignancies, in addition to prostate cancer.

specific shift to a highly pro-inflammatory PMN population (Fig. 1C, right). These findings suggest that the biggest impact on the PMN transcriptome occurs at the early stage of PCa carcinogenesis and as PCa acquires resistance to hormone-targeted therapy.

Significantly altered genes were further analyzed by Ingenuity Pathway Analysis (IPA) software (Supp Fig. 1D). The top 2 enriched canonical pathways in mCRPC PMNs compared to healthy, were: 1) glycolysis I (5 of 26 genes), and 2) 6-Phosphofructo-2-Kinase/Fructose-2,6-Bisphosphatase 4 (PFKFB4) signaling pathway (6 of 46 genes) both which are associated with altered redox signaling and glucose metabolism [23]; these findings are in support of our previous findings where we identified that BM-PCa alters redox metabolism genes in bone marrow neutrophils and increases neutrophils reactive oxygen species production (ROS) [24].

TGFβ was identified as a critical upstream mediator of several of the identified PMN gene changes including immune-regulating markers arginase 1 (*ARG1*), *WNT5B*, *IL4 receptor*, and *Cathepsin B* as well as ROS regulator, *CYBB* (Supp Fig. 2). Based on evidence of PCa-induced *CYBB* expression in human bone marrow PMNs, increased PMN release of reactive oxygen species and activation of antioxidant signaling pathways [24], we examined antioxidant protein levels in patient-derived PMNs (n = 8/group). We noticed there was reduced PMN protein content, seen by Ponceau Stain (Supp Fig. 3A); this was to be expected in terminally differentiated cells. However, this reduction was also observed in housekeeping genes, such as GAPDH (which also are metabolic enzymes) which prevented densitometry normalization. Thus, we quantified overall positivity of specific antioxidants, superoxide dismutases (SODs) and catalase per patient. There was an increase in SOD1 positive PMNs with PCa progression to metastasis and to therapy-resistant disease (Supp Fig. 3B). Specifically, there was less SOD1-positivity in PMNs of patients with metastatic diseases (~2–3 of 8 patients compared to 6 of 8 patients from localized PCa and healthy men). This suggests a potential shift in the redox metabolism of PMNs from metastatic patients.

PMNs from prostate cancer patients show a combination of mature and immature myeloid cell markers. To gain insight into PMN differentiation status, we examined known cell surface markers classically found on all PMNs, along with markers associated with immunosuppressive PMNs and pro-inflammatory, activated PMNs [14,25,26]. Cell surface markers were examined on viable peripheral blood $CD11b^{+}CD15^{+}CD16^{+}CD14^{-}$ PMNs. There were no differences in the percentage of $CD15^{+}$(granulocyte marker), $CD16^{+}$ (marker for mature granulocytes; not shown), and $CD14^{+}$ (monocyte marker) cells per diagnosis (Fig. 2A). There was a slight, though not significant, increase in LOX-1^{+} PMNs with progression to metastatic disease (i.e., comparison of localized PCa to mCSPC) indicative of an immunosuppressive phenotype. Similarly, there was a reduction in CD10-positive PMNs in all PCa patients; it was most significantly reduced in patients with bone metastases (~21 % reduction in mCSPC and mCRPC; $p < 0.01$) compared to patients with only localized PCa. PMN expression of CD10 has been associated with maturation [27], suggesting that PMN populations from PCa patients are less mature and immunosuppressive. Even still, ~50 % of PMNs from all stages expressed CD10 and fewer than ~20 % were LOX-1 positive. There was a slight reduction in CD66b, a marker of activated PMNs, on all PCa patient PMNs compared to healthy patients. However, another activation marker CD88 showed no difference when comparing healthy men with patients with localized PCa but was reduced with development of metastasis (in mCSPC). Interestingly, $CD88^{+}$ PMNs were significantly increased in mCRPC, compared to mCRPC ($p < 01$). These data highlight disease-specific changes in PMN cell surface markers that may dictate PMN function throughout PCa progression.

Collectively, these findings reveal PCa disease stage-associated alterations in canonical markers of PMN activation suggesting enhanced PMN cytotoxicity with progression of PCa to metastatic disease.

Second generation hormone therapy suppresses neutrophil cytotoxicity. The changes in gene expression and cell surface markers suggests that cytotoxity of PCa PMNs would be altered with cancer progression. To test this possibility, isolated patient PMNs (n= >17/group; Table 1) were cultured overnight with PCa cells (non-metastatic LNCaP, C42B (bone metastatic LNCaP cells), and PC3 (bone metastatic, AR-negative, PMN-resistant)) [28–30]. Patient PMNs from all disease stages induced cell death of LNCaP (~25 %) and C42B (~35–40 %), though not significantly, due to some variability between patients (Fig. 2B). In contrast, PC3 cells were resistant to PMNs from all disease stages and there was significantly more C42B cell death, induced by healthy patient PMNs (p=0.0001) and even mCRPC-PMNs ($p < 0.0001$), compared to PC3. We observed PMN cytotoxicity to PC3 (~40 % cell death) and in some cases PMNs promoted proliferation of PC3 cells (Fig. 2B).

We had previously shown PMN response to PCa to be somewhat dependent on PCa expression of STAT5, a mediator of AR signaling and target of neutrophils, such that neutrophils display targeted killing of STAT5 positive cells [31]. Our patient PMN co-culture data support the fact that there are cancer intrinsic and extrinsic factors that affect neutrophil-induced prostate cancer cell death. Patient PMNs were most cytotoxic towards the AR-positive PCa cells, however there was some variability in killing capacity such that some PMNs were both suppressive and promotive of each PCa cell line, suggesting that cytotoxicity is also dependent on PMN intrinsic factors.

The majority of all PCa patients in this study received 1st line ADT, i.e., Leuprolide, an antagonist of gonadotrophin-releasing hormone, while patients whose disease progressed (as determined by rising PSA levels) were administered 2nd generation non-steroidal anti-androgens (including abiraterone or enzalutamide) (Table 1). Previous studies have shown that, in addition to prostate epithelial cells, immune cells also express AR, which can regulate immune cell function and immune response [32,33]. Based on the diversity of ARSIs prescribed in our patient cohorts and the known functions of AR signaling in neutrophil function, we next examined PMN cytotoxicity of mCRPC patients who

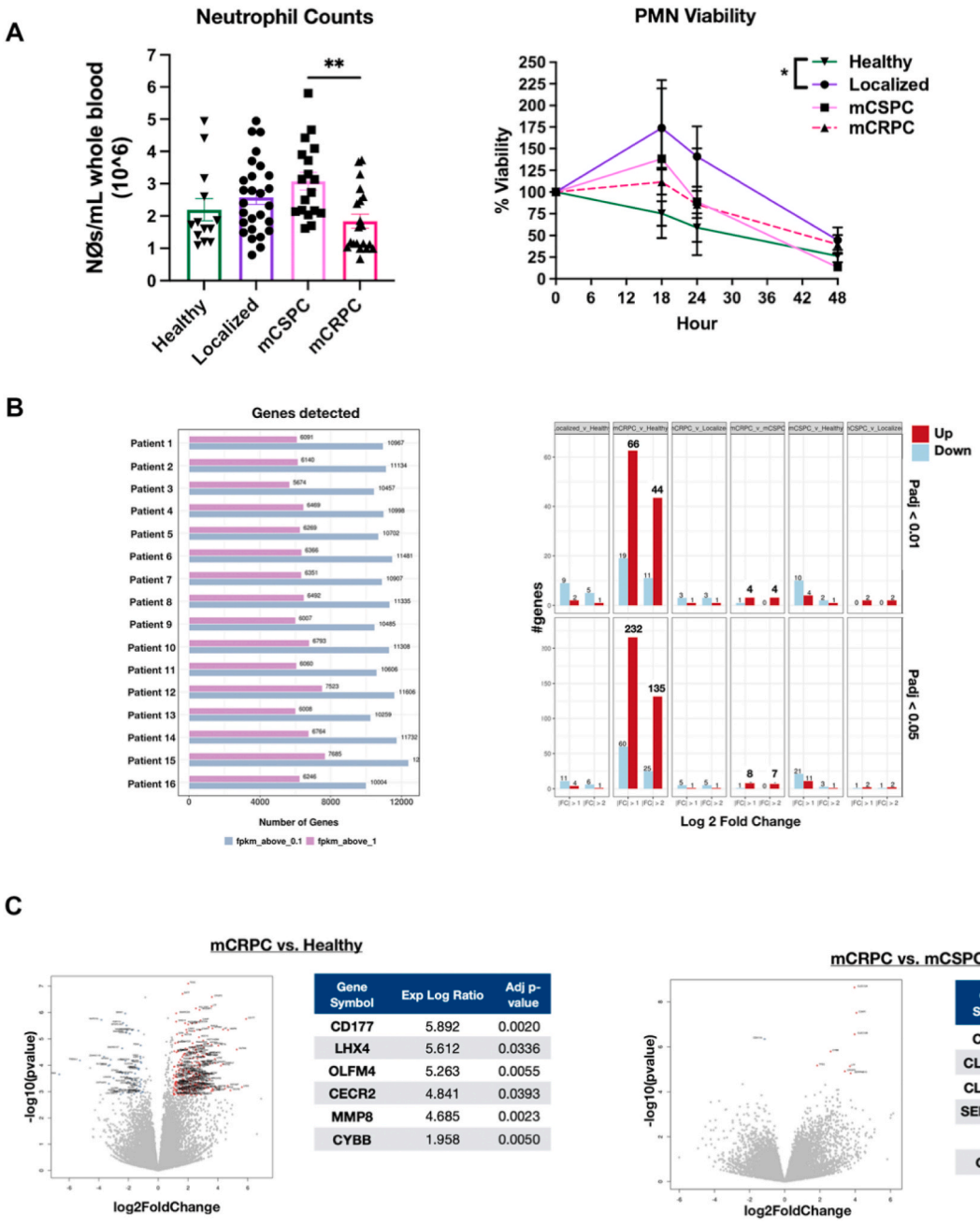

Gene Symbol	Exp Log Ratio	Adj p-value
CD177	5.892	0.0020
LHX4	5.612	0.0336
OLFM4	5.263	0.0055
CECR2	4.841	0.0393
MMP8	4.685	0.0023
CYBB	1.958	0.0050

Gene Symbol	Exp Log Ratio	Adj p-value
C3AR1	4.07	0.0002
CLEC12B	3.97	0.0011
CLEC12A	3.96	0.0000
SERPINB1	3.75	0.0192
LTF	3.70	0.0120
CYBB	2.61	0.0040

Fig. 1. Characterization of peripheral blood PMNs reveals molecular and functional parameters of PMN cytotoxicity against BM-PCa. (A) Left, PMN absolute counts per mL of blood per disease stage. One-way ANOVA was performed. **p < 0.01; Right, PMN viability per specified hours post isolation. Statistics using two-way ANOVA identified statistical significance at 18 h between healthy and localized patients; *p < 0.05 (B) RNA sequencing analysis of PCa-derived PMNs. Bulk RNA sequencing of blood PMNs was performed on an Illumina NovaSeq with paired-end 100bp reads (n per group = 4/healthy; 4/localized; 5/mCSPC; 3/mCRPC). Left, plot shows number of genes dictated per patient per fkpm. Right, number of genes significantly up-regulated (red) or down-regulated (blue) per disease stage group. Changes are separated by significance; top- ($p<0.01$), bottom- ($p<0.05$);(C) Tables show 5 most up-regulated genes when comparing most aggressive stage with non-cancer patients (mCRPC vs. healthy, left) and metastatic cohorts that differ in responsiveness to androgen therapy (mCRPC vs. mCSPC, right).

had only received 1st line ADT (Leuprolide or orchiectomy) at the time of blood collection, in comparison to PCa patients who received 2nd generation ADT, including ARSIs. We focused on these patients because they represent the most aggressive form of PCa, exhibited the most variability in PMN cytotoxicity, and these patients were represented in both cohorts of 1st line ADT vs. 2nd gen ADT. We also included one patient who received chemotherapy (Docetaxal (Doc)). Other treatment groups were excluded from the co-culture analyses (treatment demographics shown in Table 1). Interestingly, we found that PMNs from patients treated with 1st line ADT, were more cytotoxic to C42B than PMNs from patients who received 2nd generation androgen therapy (~75 % vs. ~40 %, respectively; p < 0.05) which showed impaired cytotoxicity (Fig. 2C). In total, PMNs from patients treated with 2nd generation androgen inhibition were significantly less cytotoxic than PMNs from patients treated with only 1st line ADT. Although AR is likely not the only mediator of PMN cytotoxicity, these data suggest that androgen regulation is a mediator of anti-tumor PMN response.

Bipolar androgen therapy manages BM-PCa progression and restores neutrophil immune response. Disease recurrence in PCa is typically associated with acquired resistance to androgen therapy.

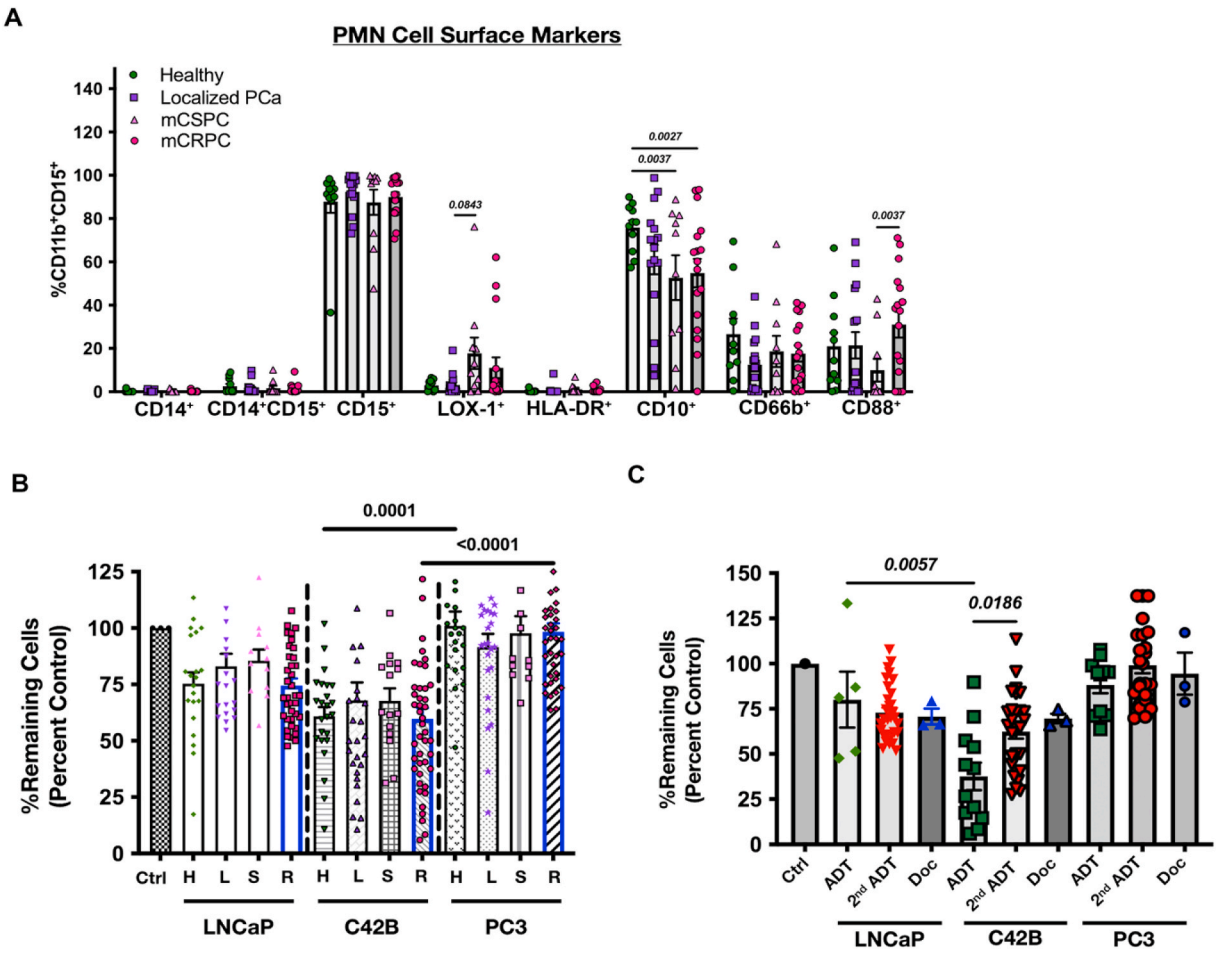

Fig. 2. Prostate cancer patient PMN surface markers and cytotoxicity. (A) FACS analysis was performed using specified cell surface markers. Plot shows percentage of marker-positive cells. Two-way ANOVA statistical analysis was performed; graph shows p-values; (B) Co-culture of patient PMNs per PCa stage with PCa cell lines (LNCaP, C42B, and PC3); 10:1 PCa to neutrophil ratio plated in triplicate. PCa cell numbers were normalized to 100 % and graph shows percent remaining PCa cells per well (technical replicates) after overnight culture with PMNs. H = healthy; L = localized; S= Castration-sensitive; R= Castration-resistant. (C) Co-culture of patient PMNs treatment with PCa cell lines (LNCaP, C42B, and PC3); graph shows percent remaining PCa cells per well (technical replicates). Ctrl = Control; ADT = 1st line androgen deprivation therapy; 2nd Gen ADT = 2nd generation androgen deprivation; Doc = docetaxel (chemotherapy).

Metastatic PCa is treated with ARSIs upon disease recurrence; however, the tumor inevitably adapts to reduced AR signaling, by reducing AR expression [34]. A previous clinical study leveraged the dynamic tumor through applied high dose testosterone to "shock" the tumor by overloading it with more testosterone than feasible to utilize (bipolar androgen therapy (BAT)), followed by cycles of 1st line ADT (GnRH antagonists/agonists) and testosterone to stabilize tumor progression [35,36]. Along these lines, we next tested the potential of using androgen regulation to manipulate neutrophil immune response *in vivo* by establishing a modified BAT study, incorporating exogenous testosterone into a mouse bone metastasis model. Male mice were administered 1st line ADT/Degarelix to deplete systemic androgen [20,21], followed by intratibial inoculation of C42B cells, and were then placed on 2nd generation ADT (i.e., enzalutamide). To examine the impact of exogenous testosterone on prostate tumor growth in bone and neutrophil function, mice were implanted with a DHT pellet, or placebo for comparison (Fig. 3A schematic). In contrast to clinical BAT studies in which patients again receive 1st line ADT after androgen treatment, we continued treating mice with 2nd generation ADT (enzalutamide) in the presence of DHT.

Surprisingly, we found that DHT alone suppressed tumor burden, demonstrated by reduced bioluminescent intensity (Fig. 3B, top graph and representative images). Although enzalutamide suppressed tumor burden more than DHT. Combined DHT and enzalutamide had the most significant impact on tumor burden compared to the control/placebo group ($p < 0.05$). Although enzalutamide suppressed tumor burden, the tumor growth rate appeared to be nearly identical when comparing sole treatment of DHT or enzalutamide. Combination DHT and enzalutamide significantly suppressed the tumor growth rate compared to DHT alone ($p < 0.01$) (Fig. 3B, bottom graph).

Next, we isolated neutrophils from the tumor bones for analyses of function, in comparison to neutrophils from saline-injected bones. Neutrophils from non-tumor limbs treated with DHT were the most viable; 75 % were still viable in serum-free media 48 h after isolation compared to 50 % from placebo-treated mice ($p < 0.0001$) and only ~25 % remaining viable cells from all tumor mice ($p < 0.0001$) compared to non-tumor bearing mice (Fig. 3C). Tumor-associated bone neutrophils (TBNs) and tumor-naïve bone neutrophils (from saline-injected tibia) were isolated from tibia and co-cultured ex vivo with C42B to examine the impact of treatment on TBN cytotoxicity. Neutrophils from both PBS and DHT-treated non-tumor bearing mice induced ~50 % cell death ($p < 0.05$). Like PMNs from patients treated with 2nd Gen ADT, cytotoxicity of TBNs from enzalutamide-treated (enza-placebo group) mice was completely diminished compared to tumor placebo-treated mice ($p < 0.001$) and tumor DHT-treated mice ($p < 0.01$). However, the addition of DHT restored TBN cytotoxicity in the presence of enzalutamide ($p < 0.0001$) (Fig. 3D).

Overall, there were very few changes in the percentages of isolated

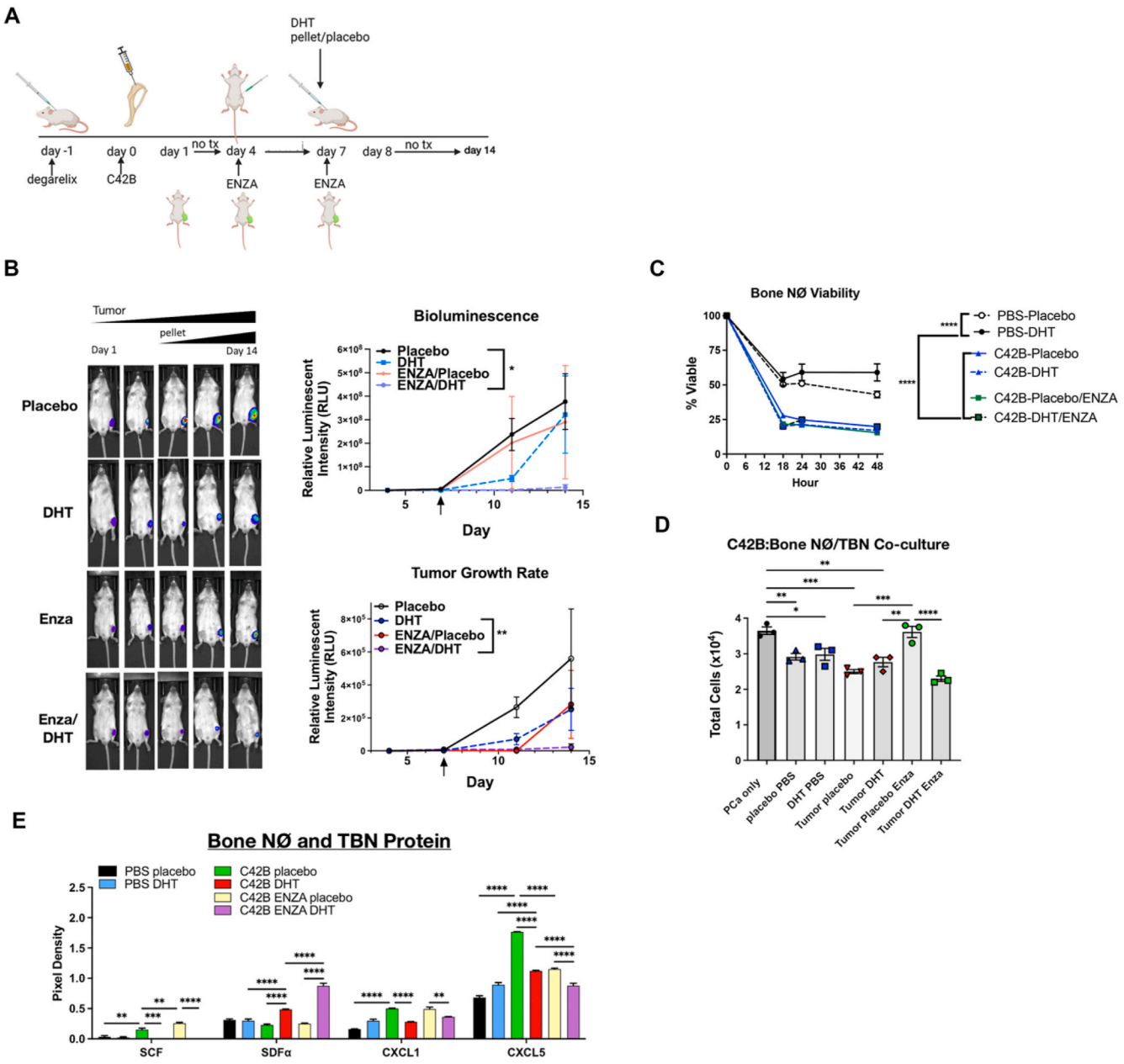

Fig. 3. In vivo and ex vivo androgen-mediated regulation of PMN cytotoxicity. (A) Schematic of pre-clinical study; generated by Biorender.com. (B) Quantitative bioluminescence imaging, representative mouse images. Top graph shows quantitation of relative luminescent intensity (RLU) in photons/cm^2/second over time. Bottom graph shows RLU normalized to bioluminescence at Day 1 post tumor inoculation. Arrows point to beginning of ADT treatment. (C) Real Time Glo MT cell viability assay of tumor-bone neutrophils (TBNs) isolated from tumor-bone at the end of study, day 14. Two-way ANOVA statistical analysis performed; ****p < 0.0001 at 18 h post-isolation. (D) C42B ex vivo co-culture with TBNs from each mouse group: placebo PBS (saline-injected mice with placebo pellet), DHT PBS (saline-injected mice with DHT pellet), tumor placebo (C42B-injected mice with placebo pellet), tumor DHT (C42B-injected mice with DHT pellet), tumor placebo Enza (C42B-injected, enzalutamide-treated, placebo pellet), and tumor DHT Enza ((C42B-injected, enzalutamide-treated, DHT pellet). For co-culture, C42B were plated in triplicate, cultured with TBNs overnight, and remaining C42B counted using Trypan Blue exclusion assay. Graph shows C42B numbers after culture with TBNs. (E) Cytokine array of TBNs. Two-ANOVA statistical analysis was performed. **p < 0.01, ***p < 0.001, ***p < 0.0001.

bone marrow myeloid cells though there were notably fewer myeloid cell numbers ((CD11b$^+$, CD45$^+$) and (CD11b$^+$, Ly6C$^+$/Ly6G$^+$)) in enzalutamide-treated mice (Supp Fig. 4A). We next examined cytokine expression in TBNs from treated groups (Fig. 3E; Supp Fig. 4B). Stem Cell Factor (SCF), a marker expressed by immature neutrophils, was significantly more expressed in TBNs from placebo-treated ($p < 0.01$) and Enza-treated mice ($p < 0.001$), compared to DHT treated; DHT-treated TBNs displayed little to no SCF suggesting that DHT may overcome tumor-mediated inhibition of neutrophil differentiation (Fig. 3E). In comparison to placebo-treated TBNs, DHT-treated TBNs exhibited higher stromal derived factor 1(SDF) alpha, the ligand that binds CXCR4, a major retention factor for neutrophils in bone marrow [37]. Notably, CXCL1 and CXCL5, cytokines shown to be important for neutrophil migration and shown to promote progression of several tumor types [38], was significantly reduced in DHT-treated TBNs compared to placebo-treated (Fig. 3E). There were few changes in myeloid-regulating growth factors, such as granulocyte colony-stimulating factor (G-CSF) and granulocyte-monocyte colony stimulating factor (GM-CSF). However, there was significantly more monocyte (M)-CSF expressed in TBNs from enza/DHT mice compared to

DHT-treated mice (Supp Fig. 4B). TBNs from mice treated with enza/DHT showed increased tumor necrosis factor alpha (TNFα) and TNF receptor expression which supported the cytotoxic and reactive response against C42B identified in ex vivo analyses (Supp Fig. 4B). Collectively, these findings suggest that high-dose testosterone therapy may alter the phenotype of tumor-bone neutrophils to support their maturation, cytotoxicity and retention in the bone microenvironment.

4. Androgen signaling regulates neutrophil cytotoxicity, viability, migration and NETosis

Our data suggests that androgen regulation of neutrophils can be leveraged to manage neutrophil anti-PCa immune response. To further test this possibility, C42B cells were co-cultured with bone marrow neutrophils isolated from C57BL/6 mice, in the presence of enzalutamide at 2 different doses (high dose-10 μM, low dose-3 μM). As previously seen, mouse neutrophils significantly killed approximately 45 % of the C42B cells. However, high dose enzalutamide completely abrogated neutrophil killing ($p < 0.05$) (Fig. 4A). To delineate which cell population was most affected by enzalutamide, we pre-treated C42B cells or neutrophils with enzalutamide prior to combining the cell populations together in culture. C42B were resistant to enzalutamide alone but pre-treatment with low-dose enzalutamide enhanced their sensitivity to neutrophil killing (Fig. 4B, left). Surprisingly, neutrophils pre-treated with low and high dose enzalutamide prior to culture with C42B were unable to induce cell death of C42B (Fig. 4B, right). This phenomenon was also seen in neutrophil-LNCaP cell cultures (Fig. 4C). These findings support our patient PMN data demonstrating that androgen inhibition of neutrophils reverses their cytotoxicity against PCa.

Although poorly understood, there is evidence that androgen signaling and specifically, AR-mediated signaling, is important for immune response [33]. To test the role of AR inhibition on neutrophil functions associated with activation, we examined neutrophil viability, migration and neutrophil extracellular trap (NET) production. Primary mouse bone marrow neutrophils were treated for 2 h with C42B-conditioned media supplemented with enzalutamide (3 μM and 10 μM) and viability was measured. Compared to control (DMSO)--treated neutrophils, both doses of enzalutamide prolonged neutrophil viability over time and there was an increase in luminescence of low dose-enzalutamide treated neutrophils in the first 6 h suggesting an increase in neutrophil numbers i.e., proliferation (Supp Fig. 5A); these results were confirmed using Trypan Blue exclusion assay of high dose enzalutamide-treated neutrophils (Supp Fig. 5B).

We next examined the impact of androgen inhibition on neutrophil migration in the context of prostate cancer [31]. Mouse bone marrow neutrophils were treated with enzalutamide or, for comparison, abiraterone, which inhibits CYP17A1 [39], an enzyme important for androgen synthesis and allowed to migrate to C42B-CM in a modified Boyden Chamber assay. Significantly more neutrophils migrated to C42B CM significantly more (~5-fold; $p < 0.01$) than to control serum-free media. Enzalutamide further enhanced neutrophil migration to C42B media (7-fold compared to CM; $p < 0.05$) but did not suppress neutrophil migration; whereas abiraterone had little to no impact on neutrophil migration to C42B factors (Supp Fig. 5C). This suggests that neutrophil migration toward BM-PCa is independent of AR signaling.

Our lab previously demonstrated that PCa induces neutrophil release of NETs [31]. To examine whether NETosis is regulated by androgen signaling, bone marrow neutrophils were treated with C42B-CM supplemented with either enzalutamide or the positive control, serum-free RPMI media supplemented with PMA to induce NET formation. Similar

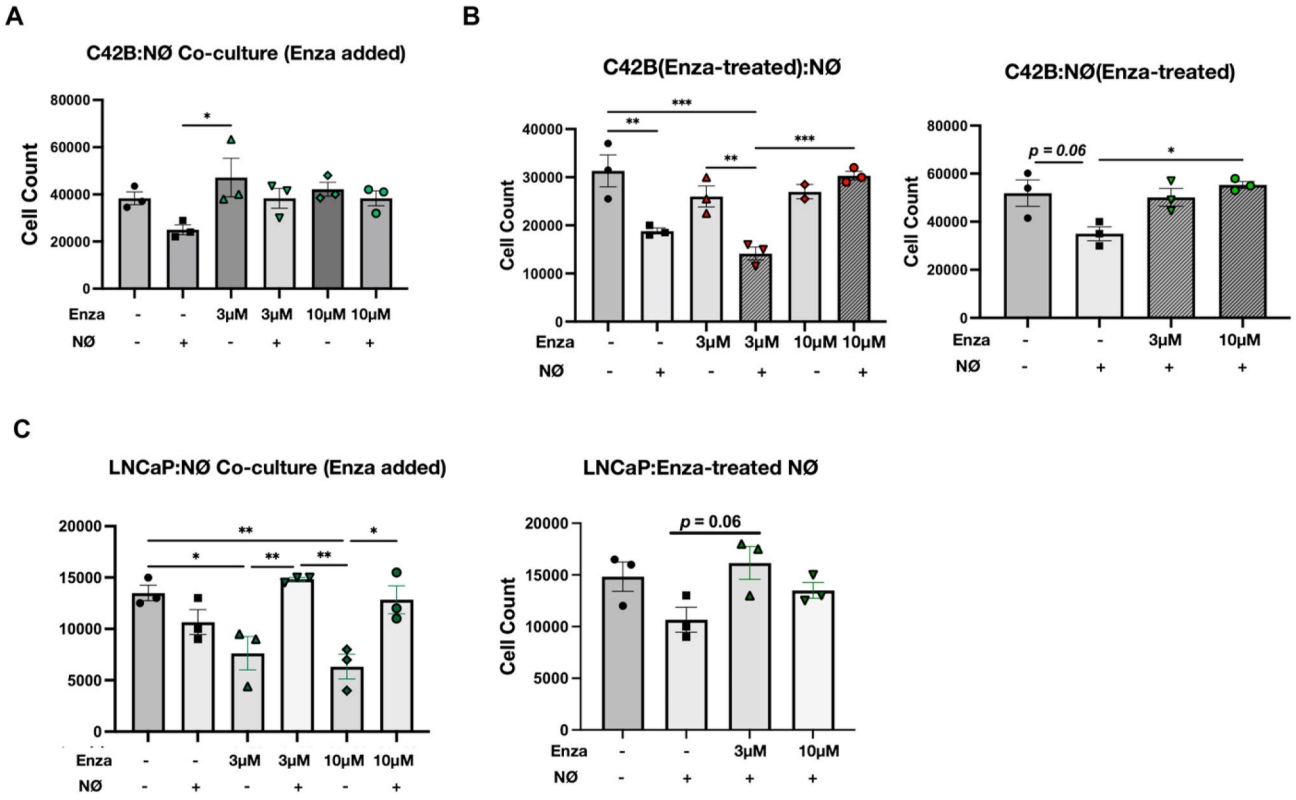

Fig. 4. Enzalutamide suppresses neutrophil cytotoxicity. (A) C42B direct co-culture with primary mouse bone marrow neutrophils. enzalutamide (Enza) was added to the culture when neutrophils were seeded. (B) Left, C42B were treated with enzalutamide (6 h) and neutrophils added for overnight culture; right, primary mouse bone marrow neutrophils were treated with enzalutamide for 30 min and then added to C42B for direct co-culture overnight. Graphs show C42B cells after overnight culture via Trypan Blue exclusion assay. (C) Left, LNCaP direct co-culture with mouse neutrophils and enzalutamide added directly to culture. Right, neutrophils were treated with enzalutamide for 30 min before addition to culture. Graphs show C42B cells after overnight culture via Trypan Blue exclusion assay. One way ANOVA statistical analysis was performed; *p < 0.05, **p < 0.01, ***p < 0.001.

to migration data, low-dose enzalutamide further enhanced NETosis (4-fold; $p<0.01$) compared to untreated neutrophils in CM (Supp Fig. 5D); high-dose enzalutamide showed no impact on NETs. These findings collectively suggest that neutrophil AR regulates neutrophil cytotoxicity and viability but is not the sole regulator of neutrophil migration and NETosis.

Second generation AR therapy regulates neutrophil gene expression *in vitro* and in patients. We next examined enzalutamide-mediated gene expression potentially contributing to neutrophil function. Based on the RNAseq results revealing TGFβ to be a mediator of PMN gene expression changes in mCRPC patients (Supp Fig. 2), we examined expression of TGFβ receptors in patient PMNs. In patients treated with 2nd Gen ADT, we observed a significant increase in PMN gene expression of the serine-threonine kinase, Type 1 TGFβ Receptor (*TβRI*), and the Type 2 TGFβ receptor, which binds TGFβ ligands (*TβRII*) (~2-fold increase of both receptors; $p < 0.05$), in comparison to patients treated with only 1st line ADT (Fig. 5A).

For validation in our preclinical models, primary mouse bone marrow neutrophils were treated with 2 doses of enzalutamide (3 μM and 10 μM) and neutrophil gene expression measured. We detected abundant levels of AR and found that enzalutamide treatment significantly reduced neutrophil AR expression (3 μM-~9-fold, $p<0.001$; 10 μm-~2-fold, $p<0.05$) compared to vehicle control (DMSO)-treated neutrophils (Fig. 5B). As seen with patient PMNs, AR inhibition increased TβRI and in a dose-dependent manner (10 μm-~3-fold, $p<0.01$); there was a slight, but significant, increase in TβRII, which binds TGFβ ligands in enzalutamide-treated neutrophils ($p<0.01$) (Fig. 5B). In addition to TGFβ receptors, we measured expression levels of TNFα, a pro-inflammatory cytokine which has been shown to be inhibited by TGFβ and neutrophil AR [40–42]. There was also a 2-fold reduction in TNFα expression by both low- ($p<0.001$) and high-dose ($p<0.01$) enzalutamide treatment. These findings suggest that AR regulates TGFβ receptor expression in neutrophils which may be significant in neutrophil function.

Neutrophil-selective- and pharmacological TβRI inhibition rescues enzalutamide-mediated suppression of function. Based on known anti-inflammatory and immunosuppressive roles of TGFβ, we next tested the importance of neutrophil TβRI expression on neutrophil cytotoxicity against BM-PCa. Primary bone marrow neutrophils were pre-treated with enzalutamide alone or in combination with RepSox, a small molecule kinase inhibitor of TβRI, and then subsequently cultured them with C42B and PC3 for comparison. Notably, inhibition of neutrophil TβRI reversed enzalutamide suppression of neutrophil cytotoxicity and significantly enhanced neutrophil-induced C42B cell death resulting in 75 % C42B cell death with RepSox/enzalutamide combination ($p<0.0001$), compared to ~50 % cell death by vehicle-treated neutrophils; ($p<0.01$) (Fig. 5C). Further, RepSox-treated neutrophils induced significant death of PC3 cells ($p<0.001$) which are resistant to

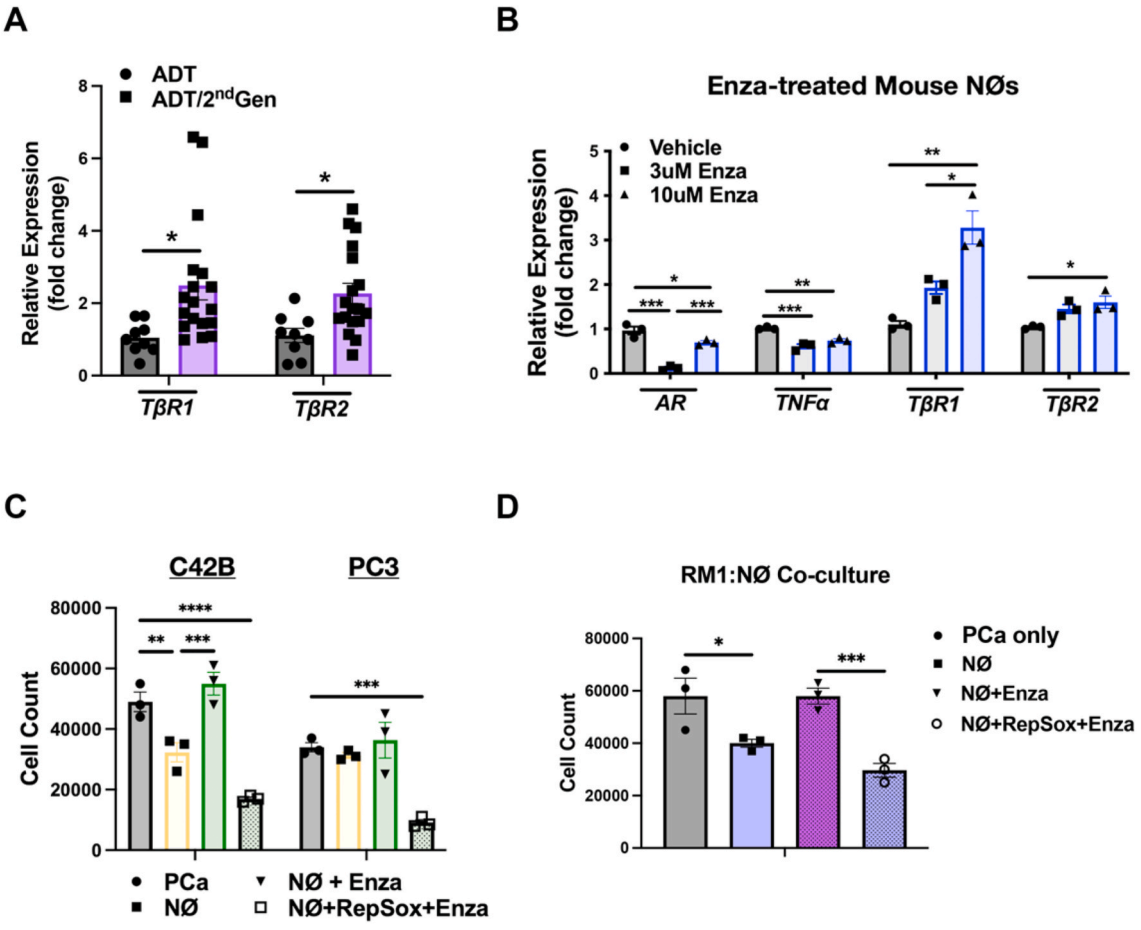

Fig. 5. ARSIs suppresses neutrophil anti-tumor response via regulation of TβR1 expression. (A) RT-qPCR of human patient PMNs treated with either 1st line androgen deprivation therapy (ADT) or 2nd generation ADT (includes all ARSIs plus 1st line ADT). (B) RealTime quantitative PCR (RT-qPCR) of mouse primary bone marrow neutrophils treated with enzalutamide. Genes profiled: androgen receptor (AR), tumor necrosis factor alpha (TNFa), transforming growth factor beta receptor 1 (TβR1). (C) C42B and PC3 co-culture assay with mouse bone marrow neutrophils pre-treated for 30 min with either RepSox (small molecule kinase inhibitor of TβR1; 5 nM), enzalutamide (3 μM) or a combination prior to addition to overnight culture. Graph shows PCa cell counts after overnight culture. (D) Mouse RM1 PCa culture with mouse neutrophils pre-treated with RepSox and/or enzalutamide for 30 min prior to addition to culture. Graph shows RM1 cell counts after overnight culture. One-way or two-way ANOVA statistical analysis were performed where appropriate. *p < 0.05, **p < 0.01, ***p < 0.001, ****p < 0.0001.

neutrophil responses. This phenomenon was also verified using mouse RM1 prostate cancer cells demonstrating that our findings are conserved between species (Fig. 5D). Collectively, these data suggest that inhibition of neutrophil AR suppresses neutrophil killing response via TβRI.

TGFβ is a pleiotropic cytokine utilized by multiple cells within the bone marrow, which complicates therapeutic intervention. To gain insight into TβRI expression in mouse bone marrow and the potential for TβRI-focused therapy, we analyzed unpublished single cell RNA sequencing data from male C57BL/6 bone marrow with a specific focus on TβRI expression in Ly6G$^+$ cells and overall TβRI expression in bone marrow cells (Supp Fig. 6A). There was TβRI expression in bone marrow neutrophils and all neutrophil subpopulations within the bone marrow (Supp Fig. 6A). However, TβRI was not expressed in all Ly6G$^+$ cells i.e., granulocytes, suggesting that TβRI expression may be more expressed in the presence of androgen inhibition and expression is low under normal conditions i.e., in normal bone marrow.

To gain additional insight into TβRI expression in PCa metastases, we performed fluorescent immunohistochemistry on matched liver and bone metastasis from FFPE samples collected in the University of Washington Rapid Autopsy Prostate Cancer program (n = 3; all who received 2nd Gen ADT), to identify TβRI$^+$ neutrophils, identified by myeloperoxidase (MPO). We found co-localization of TβRI and MPO (in

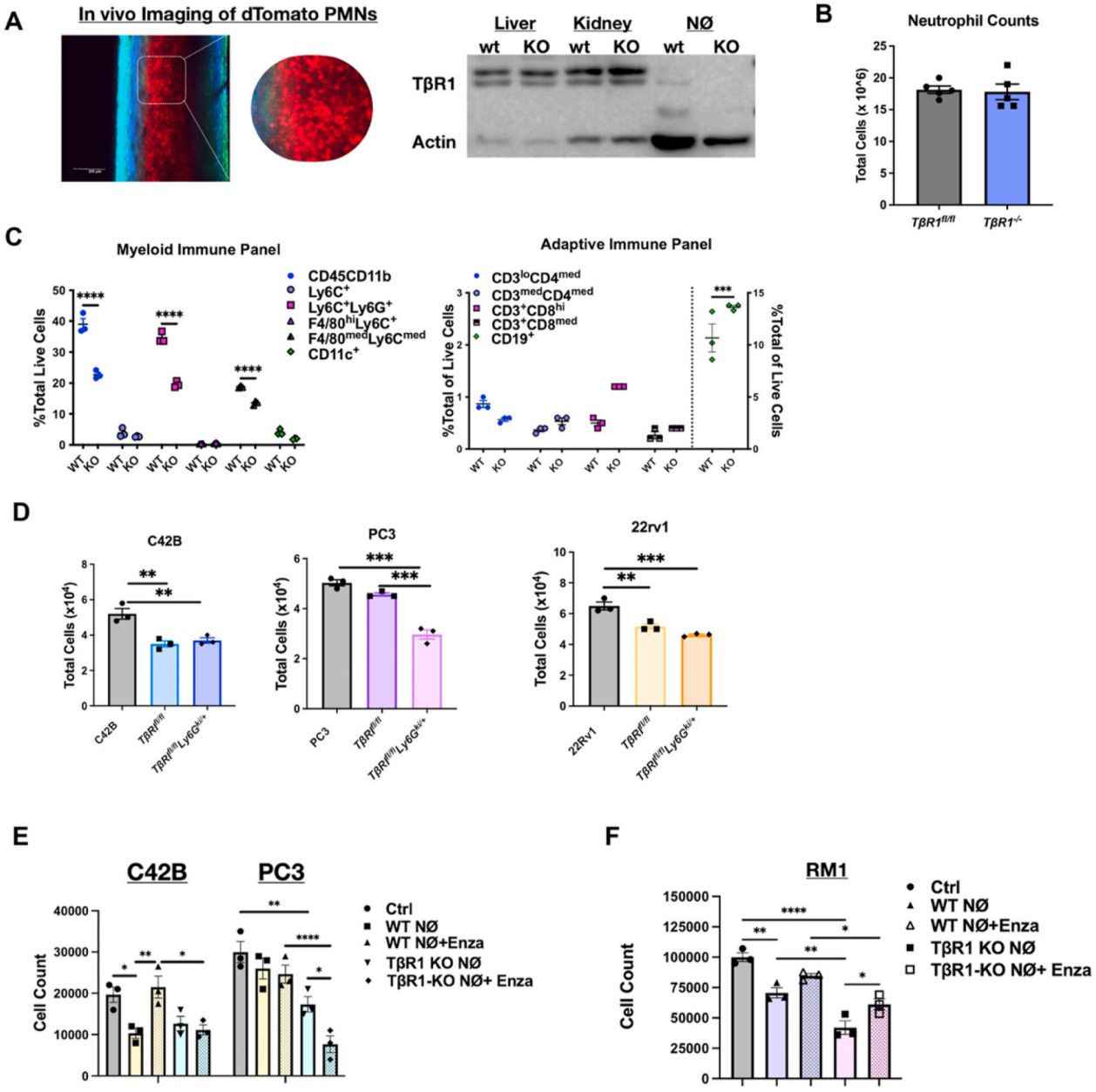

Fig. 6. Neutrophil-selective genetic deletion of TβRI rescues enzalutamide neutrophil suppression. (A) Left, two-photon microscopy of bone marrow of Catchup mouse model. Right, Western blot of TβRI in tissues from Catchup/TβRI flox/flox crossed mice. (B) Neutrophil counts post-isolation from mouse bone marrow. (C) Flow cytometry of myeloid cell markers (left) and adaptive immune markers (right) from mouse bone marrow from floxed TβRI ($T\beta RI^{fl/fl}$) and TβRI-null ($T\beta R1^{-/-}$) mice. (D) Co-culture of wildtype TβRI and TβRI-null mouse bone marrow neutrophils with BM-PCa cell lines C42B, PC3 and 22Rv1. (E) Co-culture of mouse bone marrow neutrophils in the presence of enzalutamide (Enza). C42B and PC3 co-culture assay with $T\beta RI^{fl/fl}$ and $T\beta R1^{-/-}$ mouse bone marrow neutrophils pre-treated with Enza (3 μM) prior to addition to overnight culture. Graph shows PCa cell counts after overnight culture. Two-way ANOVA statistical analysis was performed. *p < 0.05, **p < 0.01, ****p < 0.0001. (E) RM1 co-culture assay with $T\beta RI^{fl/fl}$ and $T\beta R1^{-/-}$ neutrophils pre-treated with Enza (3 μM), where shown, prior to addition to overnight culture. Graph shows PCa cell counts after overnight culture. One-way ANOVA statistical analysis was performed.

3 of 3 patients) whereas there was little to no co-localization of TβRI and MPO in the matched liver metastases (co-localization was seen in 1 of 3 patients) suggesting that TβRI-expressing neutrophils may be more conserved in prostate cancer bone metastases, compared to liver metastasis (Supp Fig. 6B).

Based on these data, we generated a neutrophil-selective TβRI knockout mouse model using the Catchup mouse model, which expresses Cre-recombinase and dTomato under the Ly6G locus (Fig. 6A, left). Ly6G is a cell surface marker specifically expressed by mouse granulocytes, which allows for a more specific targeting to neutrophils instead of all myeloid cell populations [43]. Protein analysis of multiple mouse tissues revealed a neutrophil-specific loss of TβRI protein expression, with no change in other tissues (Fig. 6A, right). There were no differences in neutrophil cell number with genetic deletion of TβRI, however there were significantly fewer myeloid cells ($CD45^{+}CD11b^{+}$) in the bone marrow (Fig. 6B). Although there appeared to be significantly fewer $Ly6G^{+}$ cells in $T\beta RI^{-/-}$ knockout mice ($p<0.0001$) (Fig. 6C, left), this was not surprising considering that the Ly6G knock-in disrupts Ly6G expression without impacting cellular function [13]. Surprisingly, there was a significant increase in $CD19^{+}$ B cells ($p<0.001$), and an increase in (though not significant) $CD8^{++}$ cells in $T\beta RI^{-/-}$ bone marrow (Fig. 6C, right) suggesting an indirect impact of neutrophil TGFβ signaling on other immune cell populations.

Next, we examined killing capacity of TβRI knockout neutrophils against BM-PCa cells (C42B, PC3, and 22Rv1). Neutrophils induced death of C42B, independently of TβRI expression as there was no difference in C42B death induced by wildtype TβRI neutrophils ($T\beta RI^{fl/fl}$) and TβRI knockout ($T\beta RI^{-/-}$) neutrophils (Fig. 6D, left). Similar to our findings using pharmacologic blockade of TβRI, $T\beta RI^{-/-}$ neutrophils induced significant cell death of PC3, neutrophil-resistant (Fig. 6D, middle; $p < 0.001$), compared to $T\beta RI^{fl/fl}$ neutrophils. Neutrophils also induced 22Rv1 death, but there was little additional impact in the absence of TβRI (Fig. 6D, right).

To examine the impact of neutrophil-selective TβRI in the context of

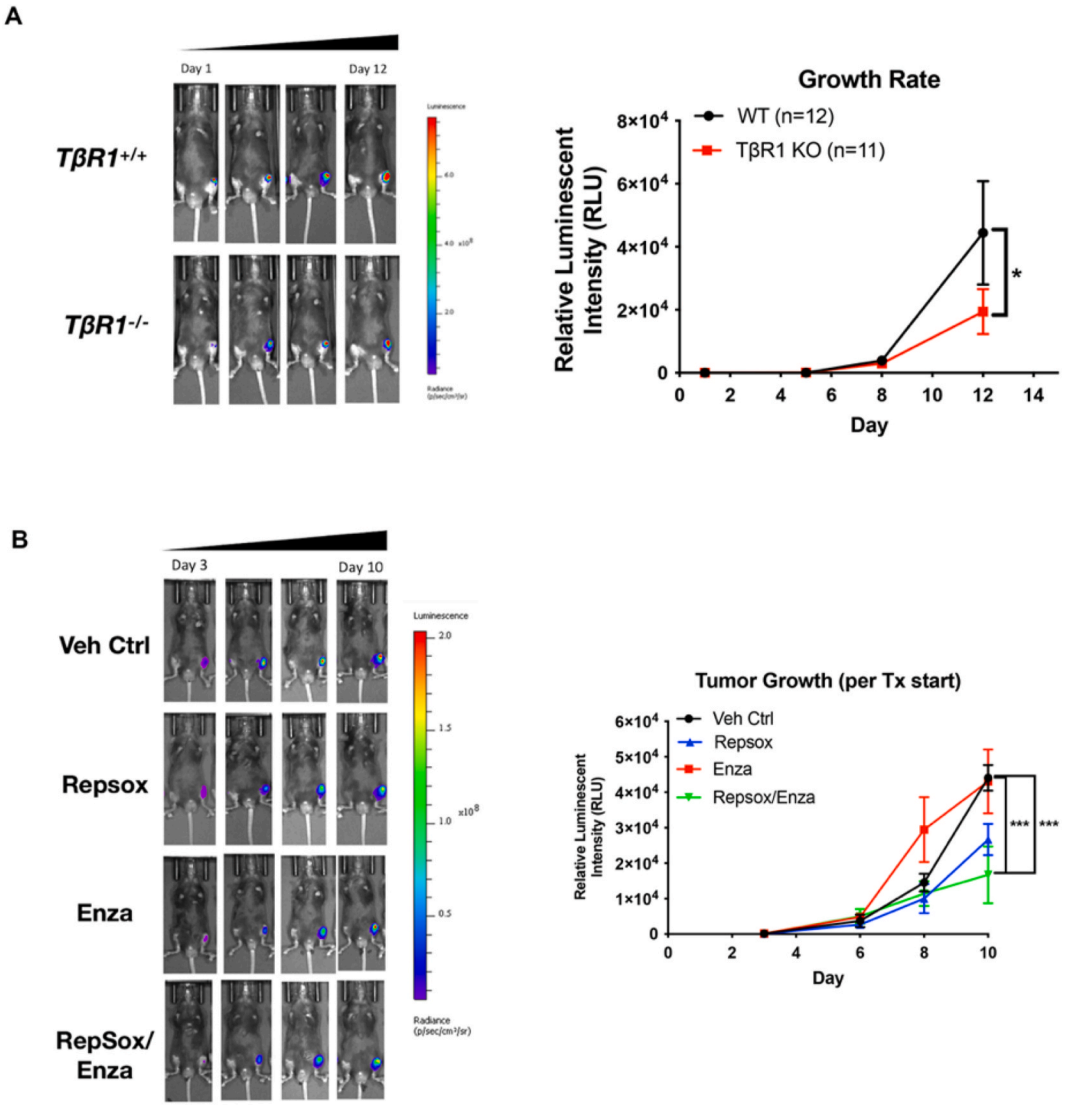

Fig. 7. Impact of neutrophil-targeted deletion of TβRI and combined TβRI/enzalutamide inhibition on BM-PCa growth. (A) RM1 intratibial bone metastasis model in TβRI KO mice. Luciferase-expressing RM1 cells were injected into tibia of 6–7 week male floxed *TβRI* (n = 12) or neutrophil-selective *TβRI*-null mice (n = 11) and tumor burden measured longitudinally for the entire study using bioluminescence imaging. Representative image (left) and bioluminescence quantitation (right, photons/cm2/sec). Two-way ANOVA statistical analysis was performed. *p < 0.05 at Day 12 of the study. (B) RM1 intratibial metastasis in preclinical therapeutic trial. Luciferase-expressing RM1 was injected intratibially in 6-week C57BL/6 mice (n = 5–7) and randomized via bioluminescence into 4 treatment groups: 1) vehicle control (DMSO), 2) RepSox (5 mg/kg), 3) enzalutamide (Enza; 10 mg/kg), 4) RepSox combined with Enza. Representative images (left) and quantitation (right). Two-way ANOVA statistical analysis was performed; graph shows significance at end of study (Veh. Ctrl vs. combo treatment and Enza vs. combo treatment) at Day 10. ***$p^{*}<0.001$.

androgen-mediated activity, we treated bone marrow neutrophils from TβRI knockout and TβRI floxed mice with low-dose enzalutamide (3 μM) (or vehicle control) prior culture with C42B and PC3 cells. As seen in our previous experiments, there was ~50 % C42B cell death induced by untreated $T\beta RI^{fl/fl}$ neutrophils which were completely suppressed by enzalutamide treatment (0 % C42B cell death by enza-treated $T\beta RI^{fl/fl}$ neutrophils; $p < 0.01$) demonstrating that enzalutamide treatment inhibits $T\beta RI^{fl/fl}$ -induced C42B cell death. In contrast, enzalutamide-treated $T\beta RI^{-/-}$ neutrophils sufficiently killed ~50 % of C42B ($p < 0.05$), (Fig. 6E). Interestingly, untreated $T\beta RI^{-/-}$ neutrophils killed ~40 % of PC3 cells ($p < 0.01$) and, further, enzalutamide-treated $T\beta RI^{-/-}$ killed ~75 % of PC3 (Fig. 6E). Additionally, mouse RM1 prostate cancer cells were cultured with TβRI knockout neutrophils in the presence of enzalutamide. Similar to human PCa, enzalutamide suppressed neutrophil killing of RM1 and this phenomenon was significantly reversed with TβRI knockout neutrophils ($p < 0.05$) compared to wild-type neutrophils (Fig. 6F). These data suggest that TβRI inhibition activates neutrophils against androgen insensitive metastatic PCa and that combined loss of TβRI and AR may enhance neutrophil response.

Last, we sought to determine whether these data translated to the prostate tumor-bone microenvironment. Luciferase-expressing RM1 cells were injected into tibia of $T\beta RI^{fl/fl}$ and $T\beta RI^{-/-}$ mice and tumor growth measured throughout the study. Based on bioluminescent changes, genetic deletion of *TβRI* in neutrophils alone significantly suppressed RM1 growth in bone (Fig. 7A). Despite these findings, it would be difficult to target TβRI inhibition solely to neutrophils in the bone microenvironment. Thus, we tested a more clinically feasible therapeutic approach and examined the impact of systemic TβRI or AR inhibition single or in combination in BM-PCa. We found that RM1 *in vivo* did not respond to enzalutamide and grew more aggressively compared to vehicle control. We observed that TβRI inhibition via RepSox appeared to suppress prostate tumor growth in bone which was reduced ~2-fold by Day 10/the end of the study ($p < 0.001$) but there was an added effect on tumor burden in the presence of enzalutamide (~2.5 fold; $p < 0.001$) (Fig. 7B).

Collectively, we have identified PMN markers, genetic changes and phenotypes that emerge with progression of prostate cancer, including development of metastasis and acquired resistance to 1st line ADT. Further, our findings strongly support the conclusion that androgen deprivation, specifically AR inhibition, increases neutrophil TβRI and suppresses their cytotoxicity against PCa (Fig. 8). Pharmacologic and genetic inhibition of neutrophil TβRI completely rescued this phenomenon. Thus, TβRI inhibition can be used to overcome neutrophil suppression and to simultaneously target both AR-responsive and AR-insensitive bone metastatic prostate cancer. Importantly, our study reveals insights from neutrophils that can be used to optimize therapeutic strategies and highlights a novel regulatory mechanism of androgen regulation in the regulation of neutrophil immune response.

5. Discussion

Androgen deprivation remains the primary therapeutic approach for treating metastatic PCa. However, patients frequently develop resistance to ADT e.g., develop CRPC and present with bone metastases. Newer cancer therapies, namely immunotherapy approaches, have had limited success for the treatment of advanced PCa. However, our lab previously identified that bone marrow neutrophils are activated to induce metastatic PCa death, highlighting a phenotype that may be utilized as a novel immunotherapy strategy for PCa patients. In this study, we investigated the impact of prostate cancer disease progression

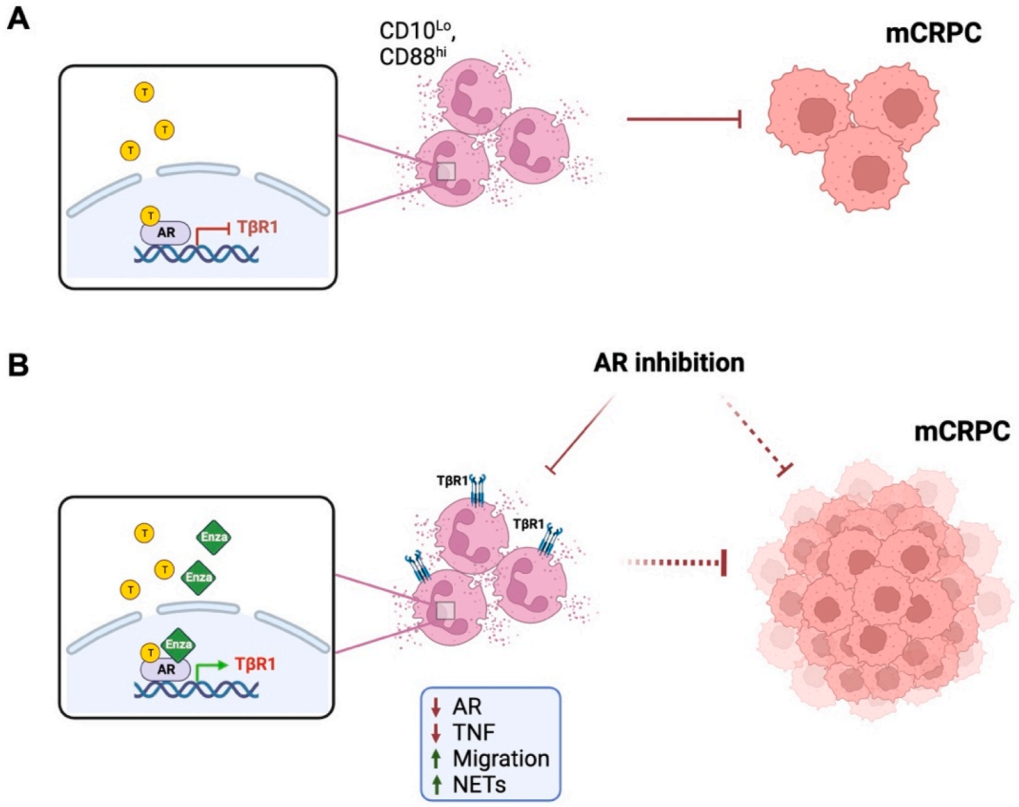

Fig. 8. AR inhibition regulates neutrophil cytotoxicity via TβR1. (A) Neutrophil function is driven, in part, by androgen signaling through AR; neutrophil AR signaling inhibits TβR1 expression and allows for neutrophil suppress of PCa growth. "T" = testosterone; "AR" = androgen receptor. mCRPC = Metastatic (bone) castration-resistant prostate cancer. (B) AR inhibition moderately suppresses metastatic PCa and promotes neutrophil TβR1 expression which inhibits neutrophil cytotoxicity. It also suppreses AR and TNF expression while increasing neutrophil migration and NETs. "Enza" = enzalutamide. Dashed lines represent inhibition of function. Created by Biorender.com.

on neutrophils to determine their potential as biomarkers for disease progression. Consequently, we identified several conclusions suggesting that: 1) classical PMN characterization is not parallel to PMN cytotoxicity against PCa, and 2) PMN anti-tumor response is highly regulated by androgen-receptor inhibition and resultant upregulation of TGFβ receptor 1.

Neutrophils/PMNs have been classically ignored in the conversation of immunotherapy due to their propensity to be short-lived terminally differentiated cells, most well characterized in infectious diseases, with emerging findings of cancer-related properties that seem to differ depending on tissue context. To date, there has been very little known of how neutrophils contribute to metastatic PCa and importantly, how neutrophils are systemically altered throughout the progression of PCa to advanced and metastatic disease. Here, we identified PCa stage-dependent differences in PMN populations that may be useful in downstream studies to develop PMN-focused therapeutic interventions. A major benefit of interrogating peripheral blood-derived PMNs as markers for disease progression is their abundance in circulation and non-invasive collection from patients. Using this to our advantage, our findings reveal that PMNs are indeed altered throughout progression and specifically, as patients transition from mCSPC to mCRPC, become more inflammatory though not necessarily more/less cytotoxic. We acknowledge that blood-derived PMNs can substantially differ in molecular pattern from bone-marrow derived PMNs, as previously discussed [44–46], which likely will be the cell populations interacting with PCa in the bone compartment. Thus, future studies are needed to compare bone marrow neutrophils throughout progression. This type of study would require substantial efforts to procure data in a non-invasive/non-painful method for patients but would provide critical data towards the characterization of PMNs in the tumor-bone environment.

Along those lines, our previous studies showed that neutrophils in bone lose their cytotoxicity as the PCa tumor progresses in bone [31]. Analysis of patient PMNs revealed a significant increase in the viability of all PCa-derived PMNs, specifically of those with localized disease compared to healthy men, suggesting the emergence of a less mature population since mature PMNs are terminally differentiated and lack mitotic ability [47]. Further, maturation markers, such as CD10, were significantly reduced with progression of disease along with CD66b. Both CD10 and CD66b have been associated with PMN maturity and are highly expressed on fully differentiated PMNs, compared to immature precursors [27,48]. There was also a significant increase in PMNs expressing CD88 (C5aR) in mCRPC compared to mCSPC. Complement C5a is a potent chemoattract for leukocyte migration, promotes granule enzyme release and oxidative burst and thus, often is associated with neutrophil activation [49]. This suggests more activated PMNs in mCRPC compared to less aggressive prostate cancer, a finding that was highly surprising. This finding was supported by RNA sequencing data which revealed a gene signature associated with neutrophil activation and degranulation; this conclusion was based upon increased expression of granule enzymes, complement receptors, and genes associated with migration and oxidative burst. Additionally, there was an increase in LOX-1 (marker for immunosuppressive cells [50]) positive cells in both cohorts of metastatic patients compared to healthy men and localized PCa. However, in total fewer than 20 % of collected PMNs expressed LOX-1 suggesting that LOX-1 expression alone may not be an appropriate marker for determining PMN function in BM-PCa. This is in consideration of previous data demonstrating bone-derived neutrophils to be both cytotoxic to PCa and immunosuppressive though further investigation would be required to determine the correlation between LOX-1 status and cytotoxicity of peripheral blood PMNs. Importantly, the changes in cell surface markers could be utilized as supportive indicators of disease stage as an accompaniment to PSA, which is sometime less reliable for more advanced PCa.

Our results showed that patient PMN cytotoxicity was not dependent on PCa disease stage, as we had initially expected. In fact, even PCa patients at the most aggressive PCa stage harbor anti-tumor PMNs. Importantly, we discovered that PMN cytotoxicity can be suppressed by 2nd generation ADT, specifically enzalutamide. Progression of PCa disease to CRPC is associated with dysregulated androgen signaling, including, but not limited to: 1) increased AR expression, 2) therapy-induced AR-activating mutations, or splice variants (e.g., AR-V7), 3) bypass of AR signaling pathways, such as STAT5 or glucocorticoid receptor (GR) signaling), and 4) AR independent signaling that occurs upon loss of AR expression (i.e., Myc activation) [34]. Based on these mechanisms of acquired resistance to 1st line ADT, ARSIs have significantly improved survival for patients with castration-resistant disease. Even still, eventually those patients become resistant to 2nd generation ADT and ~90 % develop bone metastatic disease. The findings from this study suggest that, although ARSIs may inhibit PCa growth, it may also be contributing to the development of tumor resistance to drug and anti-tumor neutrophil immune responses. Further, patients with advanced disease also are frequently treated with radiation therapy and/or chemotherapy, which both are myeloablative [51]. Thus, it is possible that the standard-of-care treatment regimen for PCa patients may, in tandem, be altering the tumor-immune microenvironment and creating a more tumor-tolerant environment. Although some of our patients received other non-androgen focused therapies, a longer more comprehensive study would be needed to examine the importance of individual therapies on neutrophil immune response in metastatic PCa.

Second generation androgen inhibition and ARSI prove to be temporarily beneficial for treating disease recurrence in CRPC however, immune cells also rely on AR for function and our data verified that neutrophils also express and utilize AR for functions that need to be interrogated further. AR is present on all PMNs and PMN precursor cells within the bone. Previous studies using conditional AR knockout mice revealed that granulopoiesis i.e., the formation of granulocytes in the bone marrow, is regulated by androgen signaling [33,52]. This evidence was supported by our findings from the modified BAT mouse and emphasizes the importance of androgens in neutrophil function. We modified this BAT protocol to reflect the treatment regimen of the mCRPC patients within our study and interrogated the impact of giving those patients exogenous testosterone upn biochemical recurrence after 2nd Generation ADT. A major limitation in the clinical translation of this work is that our hypothesis is based upon peripheral blood neutrophils which may not be representative of the bone marrow neutrophils [45]. Additionally, the C42B cancer cell line is mCRPC and has not had to go through the spontaneous development of androgen resistance prior to use in our BAT study. Nonetheless, we found that systemic DHT treatment could rescue enzalutamide-mediated suppression of neutrophil cytotoxicity and altered neutrophil markers associated with differentiation and function (Fig. 3). Specifically, AR-inhibited TBNs expressed more SCF/cKit ligand, which has been shown to be associated with immature neutrophils [53], suggesting that one method that AR impacts neutrophil function is through the suppression of neutrophil maturation. Further, AR inhibition increased neutrophil migration and proliferation, the latter being characteristic of immature (non-differentiated) neutrophils. Notably, DHT seemed to significantly suppress growth of CRPC tumors *in vivo* (in support of clinical BAT study data [35]) and this evidence, combined with TBN functional data from our mouse study suggests that androgens might be utilized to target CRPC both directly, and indirectly, through manipulation of the neutrophils in the immune microenvironment.

Based on known roles for TGFβ in the bone microenvironment [54–56] and its identification as a master regulator of PMN gene changes in PCa patients (Supp Fig. 2), we examined the role of TGFβ receptor in AR-mediated neutrophil cytotoxicity. *In vitro* preclinical data revealed that AR mediated suppression of neutrophils is predominantly caused by an increase in neutrophil TβRI expression (Fig. 8). Several studies have identified a role for TβRI in cancer immunity, namely as an immunosuppressant and a known regulator of inflammation [57–59], however, our findings emphasize a connection between neutrophil AR

and TβRI that should be investigated further for defining its role in neutrophil anti-tumor response. Canonical TGFβ signaling is propagated through ligand binding of the TβRII receptor which then forms a heterodimer complex with the kinase receptor, TβRI. TβRI activation results in phosphorylation of Smad2/3 docked at the receptor, dimerization with cytoplasmic Smad4 and translocation into the nucleus for transcriptional regulation [60]. It is unclear how androgens regulate TβRI expression. We and others have shown TGFβ receptor expression to be regulated by TGFβ signaling [55,56]. A previous study showed that AR regulates TGFβ-mediated signaling through direct association with Smad3, thereby suppressing Smad-mediated transcription. These data suggest that ARSIs disrupt the AR-Smad binding which indirectly increases TβRI expression. Recently, Paller et al. showed that TβRI inhibition using the small molecule kinase inhibitor, Galunisertib, combined with a dominant negative TβRI suppressed primary prostate tumor growth and enhanced response to enzalutamide in the neuroendocrine transgenic adenoma mouse prostate (TRAMP) model [61]. In a separate study, scRNAseq of prostate primary tumors from patients with advanced disease showed a tumor increase in TβRI expression and correlation with enzalutamide resistance demonstrating a connection between AR inhibition and TGFβ signaling in both the epithelial cancer cells as well as stromal cells [62]. In our study, we observed that AR-negative PC3 cells are resistant to neutrophil killing; however, neutrophil-specific loss of TβRI expression was able to sensitize PC3 to neutrophil killing and enzalutamide treatment suggesting that both neutrophil TβRI suppression combined with AR inhibition, significantly enhances neutrophil cytotoxicity to even the resistant BM-PCa. Further studies will be required to determine the mechanisms of TβRI and AR-mediated neutrophil function in the tumor-bone microenvironment.

Targeting TGFβ remains complicated because of the pleiotropism of TGFβ and its role in regulating an abundance of cellular processes. scRNAseq of mouse bone marrow data revealed expression of TβRI predominantly in granulocytic cells (Supp Fig. 6). Further, TβRI appears to be expressed more abundantly in neutrophils in patient bone metastases, compared to matched liver metastases (Supp Fig. 6), suggesting that systemic TβRI inhibition may be a relevant target for enhancing neutrophil anti-tumor response in bone mCRPC with limited off-target effects though this would need to be investigated further. Further, the rapid turnover of neutrophils within the bone marrow would likely require consistent TβRI inhibition, this was supported by the suppression on tumor burden in neutrophil-selective TβRI knockout mice (Fig. 6A). However, sustained combined AR and TβRI inhibition may circumvent neutrophil turnover, as we observed in the suppression on tumor growth with pharmacologic inhibitors (Fig. 6B), although extensive studies are needed to understand how neutrophil turnover would impact therapeutic intervention in the long-term.

Collectively, our data demonstrate that peripheral blood PMNs can give insight into PCa disease progression, particularly in the context of bone-metastatic disease. We identified reveal a novel finding that neutrophil anti-tumor immune response is suppressed by AR inhibition via TβRI, independently of the PMN tissue source (Fig. 8). With the benefit of current standard-of-care ADT on PCa progression, this information can be used as a two-pronged approach, leveraging TβRI as a viable target for enhancing neutrophil anti-tumor response in the presence of ADT. Importantly, we emphasize that peripheral blood PMN functional assay may be a feasible method for optimizing therapeutic intervention of mCRPC.

CRediT authorship contribution statement

Massar Alsamraae: Writing – original draft, Data curation. **Diane Costanzo-Garvey:** Writing – original draft, Data curation. **Benjamin A. Teply:** Writing – review & editing, Resources, Methodology, Conceptualization. **Shawna Boyle:** Resources. **Gary Sommerville:** Methodology, Data curation. **Zachary T. Herbert:** Formal analysis, Data curation. **Colm Morrissey:** Resources. **Alicia J. Dafferner:** Data curation. **Maher Y. Abdalla:** Methodology, Data curation. **Rachel W. Fallet:** Resources, Data curation. **Tammy Kielian:** Writing – review & editing, Resources. **Heather Jensen-Smith:** Resources, Formal analysis, Data curation. **Edson I. deOliveira:** Data curation. **Keqiang Chen:** Resources. **Ian A. Bettencourt:** Formal analysis, Data curation. **Ji Ming Wang:** Resources. **Daniel W. McVicar:** Writing – review & editing, Supervision, Resources. **Tyler Keeley:** Data curation. **Fang Yu:** Supervision, Methodology, Formal analysis. **Leah M. Cook:** Writing – review & editing, Writing – original draft, Supervision, Resources, Project administration, Methodology, Investigation, Funding acquisition, Formal analysis, Conceptualization.

Declaration of competing interest

The authors declare that they have no known competing financial interests or personal relationships that could have appeared to influence the work reported in this paper.

Acknowledgements

The authors thank Dr. Yusuke Shiozawa for kindly providing the RM1 cells and Dr. Mathias Gunzer for providing the Catchup mice used in this manuscript. LMC was supported by a Research Scholar Grant (RSG-19-127-01-CSM) from the American Cancer Society. This work was supported in part by the Flow Cytometry, Small Animal Imaging Laboratory, and Molecular Biology cores at UNMC. The authors acknowledge use of the UNMC Multiphoton Intravital & Tissue Imaging (MITI) Facility (RRID:SCR_022478) supported by P30GM127200 (NIGMS, NCN), P20GM130447 (NIGMS, CoNDA), P30CA036727 (NCI, Buffett Cancer Center), S10OD030486 (NIH), and the Nebraska Research Initiative (NRI). The UNMC Flow Cytometry Research Facility is administrated through the Office of the Vice Chancellor for Research and supported by state funds from NRI and The Fred and Pamela Buffett Cancer Center's National Cancer Institute Cancer Support Grant. Major instrumentation has been provided by the Office of the Vice Chancellor for Research, The University of Nebraska Foundation, the Nebraska Banker's Fund, and by the NIH-NCRR Shared Instrument Program. Tissue acquisition in the University of Washington Prostate Cancer Donor Rapid Autopsy Program was supported by the Pacific Northwest Prostate Cancer SPORE (P50CA97186). This research was supported, in part, by the Intramural Research Program of the NIH, National Cancer Institute, Center for Cancer Research (CCR) and Cancer Innovation Laboratory (CIL) .

Appendix A. Supplementary data

Supplementary data to this article can be found online at https://doi.org/10.1016/j.canlet.2023.216468.

References

[1] C.H. Pernar, E.M. Ebot, K.M. Wilson, L.A. Mucci, The epidemiology of prostate cancer, Cold Spring Harb Perspect Med 8 (2018).
[2] R.L. Siegel, K.D. Miller, N.S. Wagle, A. Jemal, Cancer statistics, 2023, CA A Cancer J. Clin. 73 (2023) 17–48.
[3] P.H. Viale, The American cancer society's facts & figures: 2020 edition, J Adv Pract Oncol 11 (2020) 135–136.
[4] E.M. Sebesta, C.B. Anderson, The surgical management of prostate cancer, Semin. Oncol. 44 (2017) 347–357.
[5] H. Akaza, G. Procopio, C. Pripatnanont, G. Facchini, S. Fava, D. Wheatley, K. C. Leung, M. Butt, A. Silva, L. Castillo, V. Karavasilis, A. Özatilgan, S. Hitier, E. B. Ecstein-Fraisse, M. Özguroglu, Metastatic castration-resistant prostate cancer previously treated with docetaxel-based chemotherapy: treatment patterns from the PROXIMA prospective Registry, J Glob Oncol 4 (2018) 1–12.
[6] E.M. Schaeffer, S. Srinivas, N. Adra, Y. An, D. Barocas, R. Bitting, A. Bryce, B. Chapin, H.H. Cheng, A.V. D'Amico, N. Desai, T. Dorff, J.A. Eastham, T. A. Farrington, X. Gao, S. Gupta, T. Guzzo, J.E. Ippolito, M.R. Kuettel, J.M. Lang, T. Lotan, R.R. McKay, T. Morgan, G. Netto, J.M. Pow-Sang, R. Reiter, M. Roach, T. Robin, S. Rosenfeld, A. Shabsigh, D. Spratt, B.A. Teply, J. Tward, R. Valicenti, J. K. Wong, R.A. Berardi, D.A. Shead, D.A. Freedman-Cass, NCCN guidelines(R)

insights: prostate cancer, version 1.2023, J. Natl. Compr. Cancer Netw. 20 (2022) 1288–1298.
[7] A.S. Merseburger, L.M. Krabbe, B.J. Krause, D. Bohmer, S. Perner, G.V. Amsberg, The treatment of metastatic, hormone-sensitive prostatic carcinoma, Dtsch Arztebl Int 119 (2022) 622–632.
[8] J.S. Frieling, D. Basanta, C.C. Lynch, Current and emerging therapies for bone metastatic castration-resistant prostate cancer, Cancer Control 22 (2015) 109–120.
[9] L.M. Cook, G. Shay, A. Araujo, C.C. Lynch, Integrating new discoveries into the "vicious cycle" paradigm of prostate to bone metastases, Cancer Metastasis Rev. 33 (2014) 511–525.
[10] X. Zhang, Interactions between cancer cells and bone microenvironment promote bone metastasis in prostate cancer, Cancer Commun. 39 (2019) 76.
[11] M. Alsamraae, L.M. Cook, Emerging roles for myeloid immune cells in bone metastasis, Cancer Metastasis Rev. 40 (2021) 413–425.
[12] L.W. Terstappen, J. Levin, Bone marrow cell differential counts obtained by multidimensional flow cytometry, Blood Cell 18 (1992) 311–330. ; discussion 331-312.
[13] A. Hasenberg, M. Hasenberg, L. Mann, F. Neumann, L. Borkenstein, M. Stecher, A. Kraus, D.R. Engel, A. Klingberg, P. Seddigh, Z. Abdullah, S. Klebow, S. Engelmann, A. Reinhold, S. Brandau, M. Seeling, A. Waisman, B. Schraven, J. R. Gothert, F. Nimmerjahn, M. Gunzer, Catchup: a mouse model for imaging-based tracking and modulation of neutrophil granulocytes, Nat. Methods 12 (2015) 445–452.
[14] D.F. Quail, B. Amulic, M. Aziz, B.J. Barnes, E. Eruslanov, Z.G. Fridlender, H. S. Goodridge, Z. Granot, A. Hidalgo, A. Huttenlocher, M.J. Kaplan, I. Malanchi, T. Merghoub, E. Meylan, V. Mittal, M.J. Pittet, A. Rubio-Ponce, I.A. Udalova, T. K. van den Berg, D.D. Wagner, P. Wang, A. Zychlinsky, K.E. de Visser, M. Egeblad, P. Kubes, Neutrophil phenotypes and functions in cancer: a consensus statement, J. Exp. Med. 219 (2022).
[15] E.B. Eruslanov, S. Singhal, S.M. Albelda, Mouse versus human neutrophils in cancer: a major knowledge gap, Trends Cancer 3 (2017) 149–160.
[16] F. Veglia, A. Hashimoto, H. Dweep, E. Sanseviero, A. De Leo, E. Tcyganov, A. Kossenkov, C. Mulligan, B. Nam, G. Masters, J. Patel, V. Bhargava, P. Wilkinson, D. Smirnov, M.A. Sepulveda, S. Singhal, E.B. Eruslanov, R. Cristescu, A. Loboda, Y. Nefedova, D.I. Gabrilovich, Analysis of classical neutrophils and polymorphonuclear myeloid-derived suppressor cells in cancer patients and tumor-bearing mice, J. Exp. Med. 218 (2021).
[17] A. Dobin, C.A. Davis, F. Schlesinger, J. Drenkow, C. Zaleski, S. Jha, P. Batut, M. Chaisson, T.R. Gingeras, STAR: ultrafast universal RNA-seq aligner, Bioinformatics 29 (2013) 15–21.
[18] J. Yan, G. Kloecker, C. Fleming, M. Bousamra 2nd, R. Hansen, X. Hu, C. Ding, Y. Cai, D. Xiang, H. Donninger, J.W. Eaton, G.J. Clark, Human polymorphonuclear neutrophils specifically recognize and kill cancerous cells, OncoImmunology 3 (2014), e950163.
[19] M. Cornwell, M. Vangala, L. Taing, Z. Herbert, J. Koster, B. Li, H. Sun, T. Li, J. Zhang, X. Qiu, M. Pun, R. Jeselsohn, M. Brown, X.S. Liu, H.W. Long, VIPER: visualization Pipeline for RNA-seq, a Snakemake workflow for efficient and complete RNA-seq analysis, BMC Bioinf. 19 (2018) 135.
[20] H. Taniguchi, T. Katano, K. Nishida, H. Kinoshita, T. Matsuda, S. Ito, Elucidation of the mechanism of suppressed steroidogenesis during androgen deprivation therapy of prostate cancer patients using a mouse model, Andrology 4 (2016) 964–971.
[21] A. Knutsson, S. Hsiung, S. Celik, S. Rattik, I.Y. Mattisson, M. Wigren, H.I. Scher, J. Nilsson, A. Hultgardh-Nilsson, Treatment with a GnRH receptor agonist, but not the GnRH receptor antagonist degarelix, induces atherosclerotic plaque instability in ApoE(-/-) mice, Sci. Rep. 6 (2016), 26220.
[22] M.A. Cupp, M. Cariolou, I. Tzoulaki, D. Aune, E. Evangelou, A.J. Berlanga-Taylor, Neutrophil to lymphocyte ratio and cancer prognosis: an umbrella review of systematic reviews and meta-analyses of observational studies, BMC Med. 18 (2020) 360.
[23] M. Yi, Y. Ban, Y. Tan, W. Xiong, G. Li, B. Xiang, 6-Phosphofructo-2-kinase/fructose-2,6-biphosphatase 3 and 4: a pair of valves for fine-tuning of glucose metabolism in human cancer, Mol. Metabol. 20 (2019) 1–13.
[24] D.L. Costanzo-Garvey, A.J. Case, G.F. Watson, M. Alsamraae, A. Chatterjee, R. E. Oberley-Deegan, S. Dutta, M.Y. Abdalla, T. Kielian, M.L. Lindsey, L.M. Cook, Prostate cancer addiction to oxidative stress defines sensitivity to anti-tumor neutrophils, Clin. Exp. Metastasis 39 (2022) 641–659.
[25] J. Zhou, Y. Nefedova, A. Lei, D. Gabrilovich, Neutrophils, Pmn-Mdsc, Their biological role and interaction with stromal cells, Semin. Immunol. 35 (2018) 19–28.
[26] J.I. Youn, S. Nagaraj, M. Collazo, D.I. Gabrilovich, Subsets of myeloid-derived suppressor cells in tumor-bearing mice, J. Immunol. 181 (2008) 5791–5802.
[27] O. Marini, S. Costa, D. Bevilacqua, F. Calzetti, N. Tamassia, C. Spina, D. De Sabata, E. Tinazzi, C. Lunardi, M.T. Scupoli, C. Cavallini, E. Zoratti, I. Tinazzi, A. Marchetta, A. Vassanelli, M. Cantini, G. Gandini, A. Ruzzenente, A. Guglielmi, F. Missale, W. Vermi, C. Tecchio, M.A. Cassatella, P. Scapini, Mature CD10(+) and immature CD10(-) neutrophils present in G-CSF-treated donors display opposite effects on T cells, Blood 129 (2017) 1343–1356.
[28] M.E. Kaighn, K.S. Narayan, Y. Ohnuki, J.F. Lechner, L.W. Jones, Establishment and characterization of a human prostatic carcinoma cell line (PC-3), Invest. Urol. 17 (1979) 16–23.
[29] T.T. Wu, R.A. Sikes, Q. Cui, G.N. Thalmann, C. Kao, C.F. Murphy, H. Yang, H. E. Zhau, G. Balian, L.W. Chung, Establishing human prostate cancer cell xenografts in bone: induction of osteoblastic reaction by prostate-specific antigen-producing tumors in athymic and SCID/bg mice using LNCaP and lineage-derived metastatic sublines, Int. J. Cancer 77 (1998) 887–894.
[30] J.S. Horoszewicz, S.S. Leong, E. Kawinski, J.P. Karr, H. Rosenthal, T.M. Chu, E. A. Mirand, G.P. Murphy, LNCaP model of human prostatic carcinoma, Cancer Res. 43 (1983) 1809–1818.
[31] D.L. Costanzo-Garvey, T. Keeley, A.J. Case, G.F. Watson, M. Alsamraae, Y. Yu, K. Su, C.E. Heim, T. Kielian, C. Morrissey, J.S. Frieling, L.M. Cook, Neutrophils are mediators of metastatic prostate cancer progression in bone, Cancer Immunol. Immunother. 69 (2020) 1113–1130.
[32] K.H. Chuang, S. Altuwaijri, G. Li, J.J. Lai, C.Y. Chu, K.P. Lai, H.Y. Lin, J.W. Hsu, P. Keng, M.C. Wu, C. Chang, Neutropenia with impaired host defense against microbial infection in mice lacking androgen receptor, J. Exp. Med. 206 (2009) 1181–1199.
[33] J.J. Lai, K.P. Lai, W. Zeng, K.H. Chuang, S. Altuwaijri, C. Chang, Androgen receptor influences on body defense system via modulation of innate and adaptive immune systems: lessons from conditional AR knockout mice, Am. J. Pathol. 181 (2012) 1504–1512.
[34] P.A. Watson, V.K. Arora, C.L. Sawyers, Emerging mechanisms of resistance to androgen receptor inhibitors in prostate cancer, Nat. Rev. Cancer 15 (2015) 701–711.
[35] B.A. Teply, H. Wang, B. Luber, R. Sullivan, I. Rifkind, A. Bruns, A. Spitz, M. DeCarli, V. Sinibaldi, C.F. Pratz, C. Lu, J.L. Silberstein, J. Luo, M.T. Schweizer, C.G. Drake, M.A. Carducci, C.J. Paller, E.S. Antonarakis, M.A. Eisenberger, S. R. Denmeade, Bipolar androgen therapy in men with metastatic castration-resistant prostate cancer after progression on enzalutamide: an open-label, phase 2, multicohort study, Lancet Oncol. 19 (2018) 76–86.
[36] S.R. Denmeade, J.T. Isaacs, Bipolar androgen therapy: the rationale for rapid cycling of supraphysiologic androgen/ablation in men with castration resistant prostate cancer, Prostate 70 (2010) 1600–1607.
[37] R.C. Furze, S.M. Rankin, Neutrophil mobilization and clearance in the bone marrow, Immunology 125 (2008) 281–288.
[38] C.S. Johnson, L.M. Cook, Osteoid cell-derived chemokines drive bone-metastatic prostate cancer, Front. Oncol. 13 (2023), 1100585.
[39] Y. Rehman, J.E. Rosenberg, Abiraterone acetate: oral androgen biosynthesis inhibitor for treatment of castration-resistant prostate cancer, Drug Des. Dev. Ther. 6 (2012) 13–18.
[40] S.B. Coffelt, M.D. Wellenstein, K.E. de Visser, Neutrophils in cancer: neutral no more, Nat. Rev. Cancer 16 (2016) 431–446.
[41] E.N. Benveniste, L.P. Tang, R.M. Law, Differential regulation of astrocyte TNF-alpha expression by the cytokines TGF-beta, IL-6 and IL-10, Int. J. Dev. Neurosci. 13 (1995) 341–349.
[42] K.Y. Ryu, G.S. Cho, H.Z. Piao, W.K. Kim, Role of TGF-beta in survival of phagocytizing microglia: autocrine suppression of TNF-alpha production and oxidative stress, Exp Neurobiol 21 (2012) 151–157.
[43] J.X. Wang, A.M. Bair, S.L. King, R. Shnayder, Y.F. Huang, C.C. Shieh, R. J. Soberman, R.C. Fuhlbrigge, P.A. Nigrovic, Ly6G ligation blocks recruitment of neutrophils via a beta2-integrin-dependent mechanism, Blood 120 (2012) 1489–1498.
[44] M. Palomino-Segura, J. Sicilia, I. Ballesteros, A. Hidalgo, Strategies of neutrophil diversification, Nat. Immunol. 24 (2023) 574–584.
[45] I. Ballesteros, A. Rubio-Ponce, M. Genua, E. Lusito, I. Kwok, G. Fernandez-Calvo, T. E. Khoyratty, E. van Grinsven, S. Gonzalez-Hernandez, J.A. Nicolas-Avila, T. Vicanolo, A. Maccataio, A. Benguria, J.L. Li, J.M. Adrover, A. Aroca-Crevillen, J. A. Quintana, S. Martin-Salamanca, F. Mayo, S. Ascher, G. Barbiera, O. Soehnlein, M. Gunzer, F. Ginhoux, F. Sanchez-Cabo, E. Nistal-Villan, C. Schulz, A. Dopazo, C. Reinhardt, I.A. Udalova, L.G. Ng, R. Ostuni, A. Hidalgo, Co-Option of neutrophil fates by tissue environments, Cell 183 (2020) 1282–1297 e1218.
[46] R. Grieshaber-Bouyer, F.A. Radtke, P. Cunin, G. Stifano, A. Levescot, B. Vijaykumar, N. Nelson-Maney, R.B. Blaustein, P.A. Monach, P.A. Nigrovic, C. ImmGen, The neutrotime transcriptional signature defines a single continuum of neutrophils across biological compartments, Nat. Commun. 12 (2021) 2856.
[47] R. Sumagin, Emerging neutrophil plasticity: terminally differentiated cells no more, J. Leukoc. Biol. 109 (2021) 473–475.
[48] S. Prausmuller, G. Spinka, S. Stasek, H. Arfsten, P.E. Bartko, G. Goliasch, M. Hulsmann, N. Pavo, Neutrophil activation/maturation markers in chronic heart failure with reduced ejection fraction, Diagnostics 12 (2022).
[49] R.F. Guo, P.A. Ward, Role of C5a in inflammatory responses, Annu. Rev. Immunol. 23 (2005) 821–852.
[50] T. Condamine, G.A. Dominguez, J.I. Youn, A.V. Kossenkov, S. Mony, K. Alicea-Torres, E. Tcyganov, A. Hashimoto, Y. Nefedova, C. Lin, S. Partlova, A. Garfall, D. T. Vogl, X. Xu, S.C. Knight, G. Malietzis, G.H. Lee, E. Eruslanov, S.M. Albelda, X. Wang, J.L. Mehta, M. Bewtra, A. Rustgi, N. Hockstein, R. Witt, G. Masters, B. Nam, D. Smirnov, M.A. Sepulveda, D.I. Gabrilovich, Lectin-type oxidized LDL receptor-1 distinguishes population of human polymorphonuclear myeloid-derived suppressor cells in cancer patients, Sci Immunol 1 (2016).
[51] M. Sabloff, S. Chhabra, T. Wang, C. Fretham, N. Kekre, A. Abraham, K. Adekola, J. J. Auletta, C. Barker, A.M. Beitinjaneh, C. Bredeson, J.Y. Cahn, M.A. Diaz, C. Freytes, R.P. Gale, S. Ganguly, U. Gergis, E. Guinan, B.K. Hamilton, S. Hashmi, P. Hematti, G. Hildebrandt, L. Holmberg, S. Hong, H.M. Lazarus, R. Martino, L. Muffly, T. Nishihori, M.A. Perales, J. Yared, S. Mineishi, E.A. Stadtmauer, M. C. Pasquini, A.W. Loren, Comparison of high doses of total body irradiation in myeloablative conditioning before hematopoietic cell transplantation, Biol. Blood Marrow Transplant. 25 (2019) 2398–2407.
[52] N.D. McDonnell, R.B. Livingston, Severe reversible neutropenia following treatment of prostate cancer with flutamide, J. Urol. 151 (1994) 1353–1354.
[53] C.M. Rice, L.C. Davies, J.J. Subleski, N. Maio, M. Gonzalez-Cotto, C. Andrews, N. L. Patel, E.M. Palmieri, J.M. Weiss, J.M. Lee, C.M. Annunziata, T.A. Rouault, S. K. Durum, D.W. McVicar, Tumour-elicited neutrophils engage mitochondrial

metabolism to circumvent nutrient limitations and maintain immune suppression, Nat. Commun. 9 (2018) 5099.
[54] A. Araujo, L.M. Cook, C.C. Lynch, D. Basanta, An integrated computational model of the bone microenvironment in bone-metastatic prostate cancer, Cancer Res. 74 (2014) 2391–2401.
[55] L.M. Cook, J.S. Frieling, N. Nerlakanti, J.J. McGuire, P.A. Stewart, K.L. Burger, J. L. Cleveland, C.C. Lynch, Betaglycan drives the mesenchymal stromal cell osteogenic program and prostate cancer-induced osteogenesis, Oncogene 38 (2019) 6959–6969.
[56] L.M. Cook, A. Araujo, J.M. Pow-Sang, M.M. Budzevich, D. Basanta, C.C. Lynch, Predictive computational modeling to define effective treatment strategies for bone metastatic prostate cancer, Sci. Rep. 6 (2016), 29384.
[57] L. Yang, Y. Pang, H.L. Moses, TGF-beta and immune cells: an important regulatory axis in the tumor microenvironment and progression, Trends Immunol. 31 (2010) 220–227.
[58] A.L. Smith, T.P. Robin, H.L. Ford, Molecular pathways: targeting the TGF-beta pathway for cancer therapy, Clin. Cancer Res. 18 (2012) 4514–4521.
[59] M. Archer, N. Dogra, N. Kyprianou, Inflammation as a driver of prostate cancer metastasis and therapeutic resistance, Cancers 12 (2020).
[60] K.A. Brown, J.A. Pietenpol, H.L. Moses, A tale of two proteins: differential roles and regulation of Smad2 and Smad3 in TGF-beta signaling, J. Cell. Biochem. 101 (2007) 9–33.
[61] C. Paller, H. Pu, D.E. Begemann, C.A. Wade, P.J. Hensley, N. Kyprianou, TGF-beta receptor I inhibitor enhances response to enzalutamide in a pre-clinical model of advanced prostate cancer, Prostate 79 (2019) 31–43.
[62] M.X. He, M.S. Cuoco, J. Crowdis, A. Bosma-Moody, Z. Zhang, K. Bi, A. Kanodia, M. J. Su, S.Y. Ku, M.M. Garcia, A.R. Sweet, C. Rodman, L. DelloStritto, R. Silver, J. Steinharter, P. Shah, B. Izar, N.C. Walk, K.P. Burke, Z. Bakouny, A.K. Tewari, D. Liu, S.Y. Camp, N.I. Vokes, K. Salari, J. Park, S. Vigneau, L. Fong, J.W. Russo, X. Yuan, S.P. Balk, H. Beltran, O. Rozenblatt-Rosen, A. Regev, A. Rotem, M. E. Taplin, E.M. Van Allen, Transcriptional mediators of treatment resistance in lethal prostate cancer, Nat. Med. 27 (2021) 426–433.